Sedimentary Geology 223 (2010) 334–359

Contents lists available at ScienceDirect

Sedimentary Geology

journal homepage: www.elsevier.com/locate/sedgeo

Tectonic and eustatic control on a mixed siliciclastic–carbonate platform during the Late Oxfordian–Kimmeridgian (La Rochelle platform, western France)

Damien Carcel *, Claude Colombié, Fabienne Giraud, Bernard Courtinat

Université de Lyon, F-69622 Lyon, France
Université Lyon 1, Villeurbanne, CNRS, UMR 5125 PEPS, France

ARTICLE INFO

Article history:
Received 4 February 2009
Received in revised form 21 November 2009
Accepted 27 November 2009

Keywords:
Facies analysis
Micropaleontology
Depositional sequences
Mixed carbonate–siliciclastic platform
Kimmeridgian
Western France

ABSTRACT

Boreal and Tethyan realms of Western Europe present significant sedimentological, paleontological, and stratigraphic differences. The purpose of this study is to constrain regional versus global controls on the dynamics of a sedimentary system located at the interface of these two realms in order to better understand the origin of their differences. Detailed sedimentological, palynofacies and calcareous nannofossil analyses were performed on two sections from the La Rochelle platform (western France). The Pas section includes part of the Late Oxfordian and Early Kimmeridgian, and the Rocher d'Yves section is assigned to the Late Kimmeridgian. They correspond to monotonous marl–argillaceous limestone alternations. Limestones are essentially mudstones with echinoderms, bivalves and foraminifera that suggest low-energy, open-marine conditions. Highly bioclastic and/or peloidal deposits occur commonly, and show wackestones to wackepack-grainstones textures. These deposits indicate frequent high-energy events, and are interpreted as storm deposits. Marls dominate in the most proximal depositional environments, while calcareous deposits are more important in more distal environments. The Rocher d'Yves section is globally more marly than the Pas section, suggesting a more proximal setting. Palynofacies are dominated by woody particles, suggesting shallow-water, proximal depositional environments. Calcareous nannofossils are ascidian spicules, coccoliths, and schizospheres. *Watznaueria britannica* dominate calcareous nannofossil assemblages in the Pas section. The Rocher d'Yves assemblages are quasi-exclusively composed of *Cyclagelosphaera margerelii*, and indicate more proximal paleoenvironments than those of the Pas section. Different orders of depositional sequences are defined, with sequence boundaries corresponding to the most rapid relative sea-level falls. They are hierarchically stacked, and correlate, on the basis of ammonite zones, with the sequences of contemporaneous sections from Tethyan and boreal realms. The stacking pattern of these sequences suggests an orbital control on sedimentation. Small-, medium- and large-scale sequences correspond to precession (20 ky) cycles and to 100 ky and 400 ky eccentricity cycles, respectively. The elementary sequences have durations shorter than 20 ky. The Kimmeridgian was a period of global sea-level rise that ended in the Late Kimmeridgian. More proximal depositional environments in the Rocher d'Yves section (Late Kimmeridgian) than in the Pas section (Early Kimmeridgian) imply a progradation of the La Rochelle platform during the Kimmeridgian. This progradation resulted from a slowdown of the subsidence in the Aquitaine Basin during the Kimmeridgian, corresponding to the first steps of Atlantic Ocean opening. High-frequency cycles on the La Rochelle platform formed in sync with Milankovitch orbital cycles, while tectonics controlled the formation of the low-frequency cycles.

1. Introduction

The Kimmeridgian (Late Jurassic, 155.6–150.8 Ma, Ogg et al., 2008) of western Europe was a warm period (Lécuyer et al., 2003), with aridification on land throughout (Abbink et al., 2001). The Jurassic was a tectonically relatively stable period in western Europe. The Kimmeridgian, however, recorded the first extensional tectonic movements that preceded North Atlantic Ocean opening during the Cretaceous (Montadert and Winnock, 1971). Late Jurassic ammonite fauna define two distinctive paleobiogeographic areas in western Europe (Atrops et al., 1993): the boreal and the Tethyan realms (Fig. 1). This provincialism is probably of climatic origin (Cariou and Hantzpergue, 1997). This boreal/Tethyan distinction is present in the Late Jurassic chronostratigraphic chart of Ogg et al. (2008) (Fig. 2). This chart shows ammonite zones for the boreal and the Tethyan realms. The durations of the ammonite zones are calculated according to the absolute ages of Gradstein et al. (1994). The Ogg et al. (2008) chart also contains a sequence-stratigraphic interpretation for both

* Corresponding author. Université de Lyon, F-69622, Lyon, France.
E-mail address: damien.carcel@gmail.com (D. Carcel).

0037-0738/$ – see front matter
doi:10.1016/j.sedgeo.2009.11.018

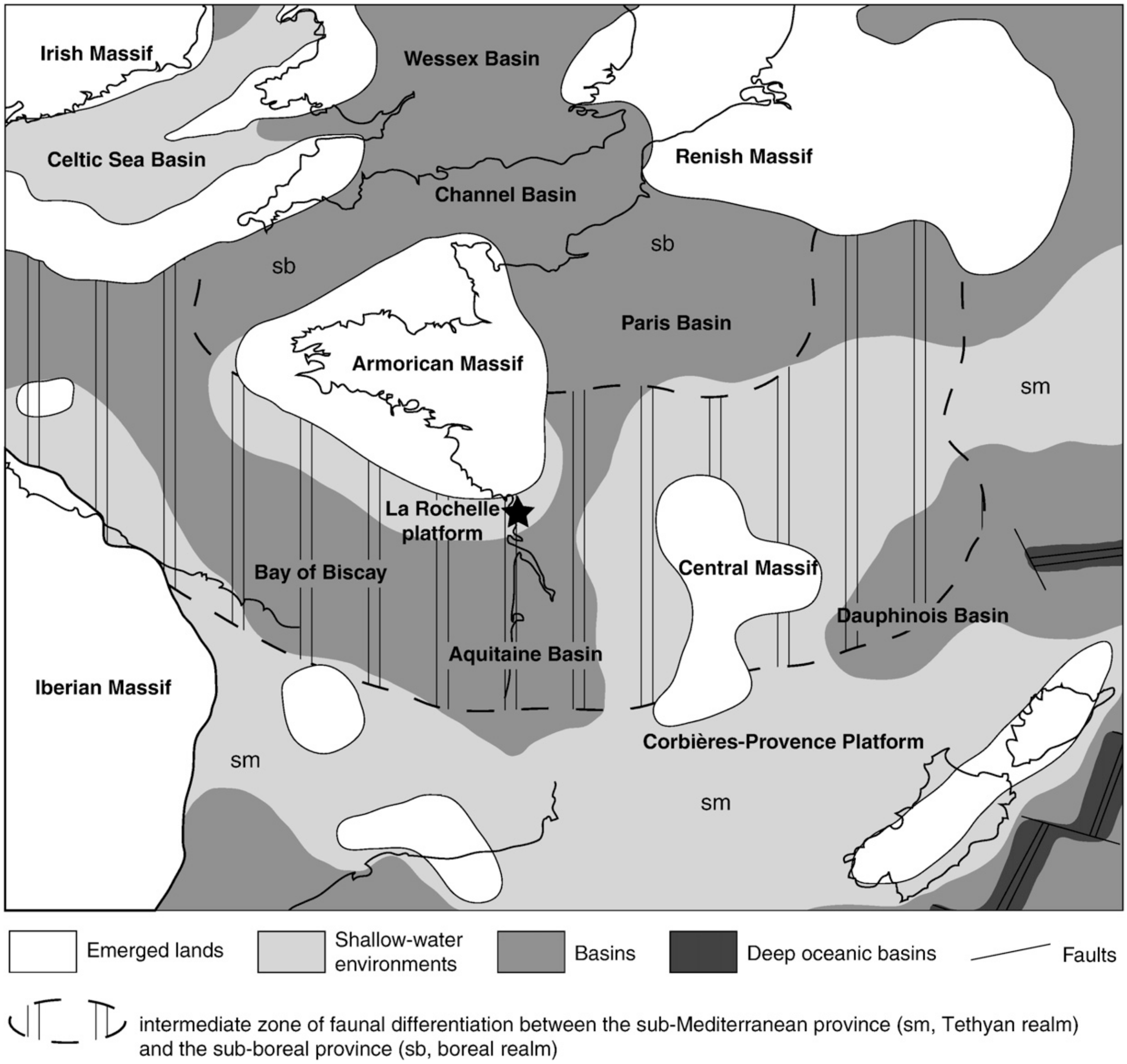

Fig. 1. Paleogeography of western Europe during the Early Kimmeridgian (after Thierry, 2000, and Cariou and Hantzpergue, 1997). The star corresponds to the location of the sections.

realms. Second- and third-order sequence boundaries and maximum-flooding surfaces are located according to the ammonite zones (Fig. 2). Sequence-stratigraphic interpretations differ between the boreal and the Tethyan realms. The Kimmeridgian contains seven boreal third-order sequences and five Tethyan ones, and the second-order maximum-flooding surfaces do not correspond with each other. Colombié and Rameil (2007) suggest that these discrepancies have a tectonic origin. The purpose of this study is to define the controlling factors on the dynamics of a sedimentary system located at the boundary between the boreal and the Tethyan realms, in order to better understand the origin of their differences.

The mixed carbonate–siliciclastic platform of La Rochelle (Fig. 1), located between the sub-boreal and the sub-Mediterranean provinces (Hantzpergue, 1991a), was selected for this work. Various studies have been carried out on this platform, but these only concern biostratigraphy (Normand, 1970; Hantzpergue, 1979, 1989, 1991a,b), regional geology (Normand, 1971; Cariou, 1972; Hantzpergue, 1984, 1985a,b, 1988, 1993, 1995), and paleontology (Lafuste, 1955; Delfaud and Servant, 1971; Fürsich and Oschmann, 1986; Olivier et al., 2003, 2008). Two sections are chosen: the Pas and the Rocher d'Yves sections, dated from Late Oxfordian–Early Kimmeridgian and from Late Kimmeridgian, respectively. The Rocher d'Yves section includes the "virgulian" facies, which corresponds to marls with a great abundance of *Nanogyra virgula* oysters (Hantzpergue, 1988). This facies also characterises the Late Kimmeridgian of the Paris Basin, the Channel Basin, and the Wessex Basin (Fig. 1). Jacquin et al. (1998) interpreted this facies like the most open-marine facies of the Paris Basin and the Wessex Basin.

This work is based on a multidisciplinary approach (sedimentology, palynofacies, and calcareous nannofossil analyses) that allows an accurate definition of depositional environments and construction of a facies model. A high-resolution sequential interpretation allows a precise stratigraphic correlation of the studied sections with other boreal and Tethyan sections. This narrow spatial and temporal framework then permits the controls on platform dynamics to be defined.

2. Geological setting

The Pas and Rocher d'Yves sections are located near La Rochelle, in western France (Fig. 3), and are 53 and 9 m thick, respectively. The Pas section is located around 6 km north of La Rochelle. It extends from Pas de l'Assassin to Pointe du Plomb. The Rocher d'Yves section is located about 16 km south of La Rochelle. The two sections, constantly eroded by the ocean, exhibit fresh outcrops that allow detailed observations.

The Pas and Rocher d'Yves sections are dated by ammonites from the Late Jurassic (Fig. 2). The Pas section includes the upper part of the

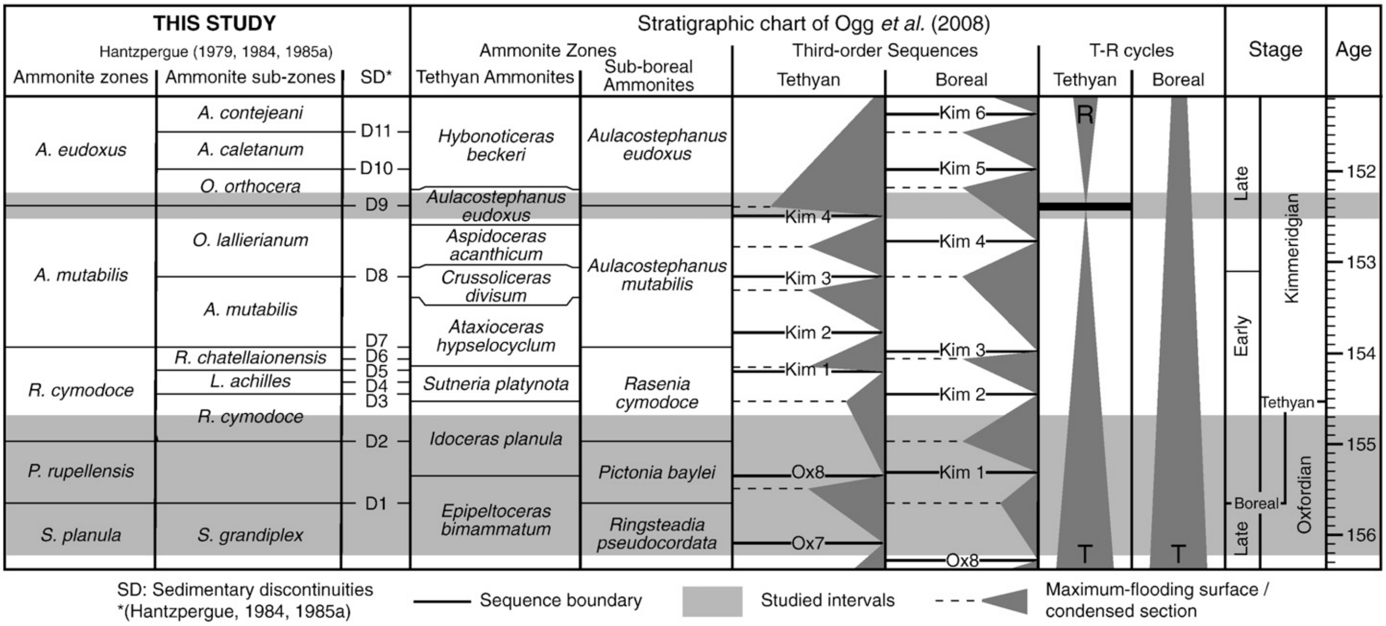

Fig. 2. Ammonite biozonation of the terminal Oxfordian and the Kimmeridgian of western France and for the boreal and Tethyan realms, Tethyan and boreal third- and second-order sequences (indicated as "Sequences" and "T–R cycles," respectively), and stratigraphic location (in grey) of the studied intervals.

planula Zone (Late Oxfordian), the *rupellensis* Zone and the lower part of the *cymodoce* Zone (Early Kimmeridgian) (Hantzpergue, 1979). The Rocher d'Yves section is located at the boundary between the *mutabilis* and the *eudoxus* Zones (Late Kimmeridgian). Hantzpergue (1984, 1985a) identified 11 sedimentary discontinuities during the Kimmeridgian, numbered D1 to D11 (Fig. 2). These discontinuities are present in most of western European basins. Except for D4 and D6, they all correspond to ammonite zone boundaries. The Pas section includes D1 and D2, and the Rocher d'Yves section contains D9. Hantzpergue (1991a, 1993, 1995) interpreted D1, D2, and D9 as third-order sequence boundaries. However, according to the sequence-stratigraphic chart of Ogg et al. (2008), D1 and D2 correspond to third-order maximum-flooding surfaces of boreal sequences (Fig. 2); D9 corresponds to the maximum-flooding surface of the Tethyan Kim 4 sequence.

The Pas and Rocher d'Yves sections were located on the La Rochelle platform (Fig. 1). This platform was a mixed carbonate-siliciclastic platform that developed south of the Armorican Massif and north of the Aquitaine Basin (Hantzpergue and Maire, 1981). Both sections

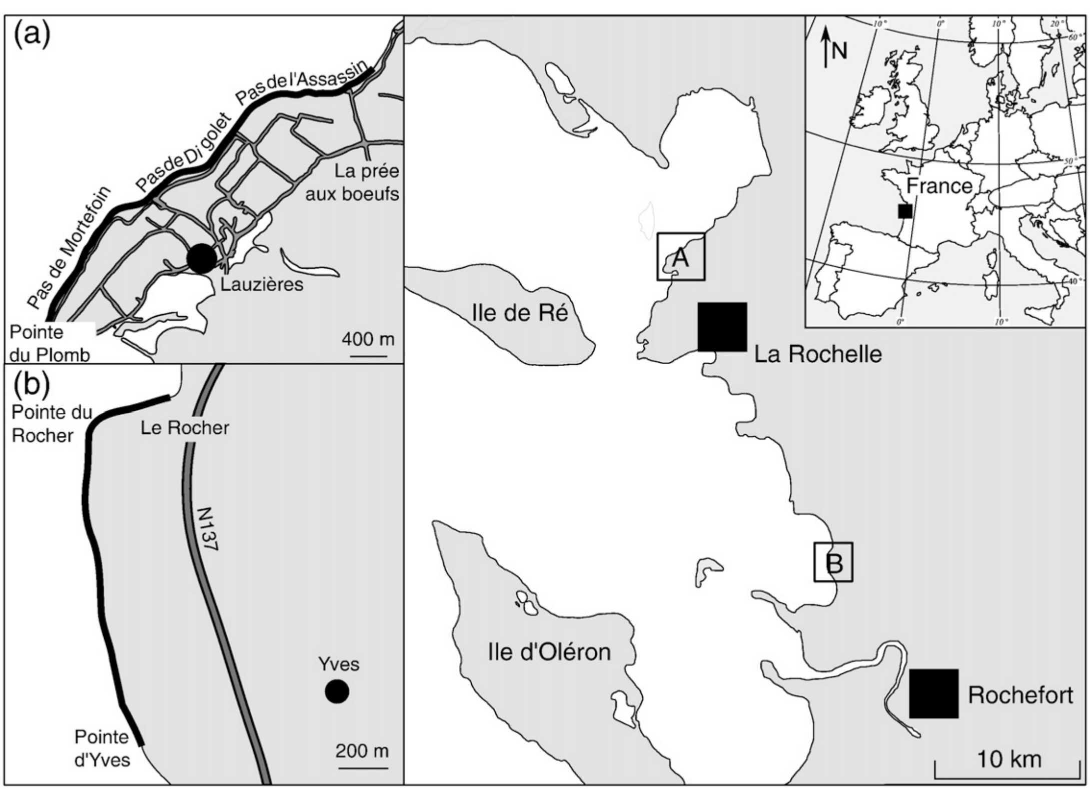

Fig. 3. Geographic location of the studied sections: the Pas section north of La Rochelle, next to the paths "Pas de l'Assassin," "Pas de Digolet," and "Pas de Mortefoin" (a), and the Rocher d'Yves section to the south (b). Sections are indicated by bold lines.

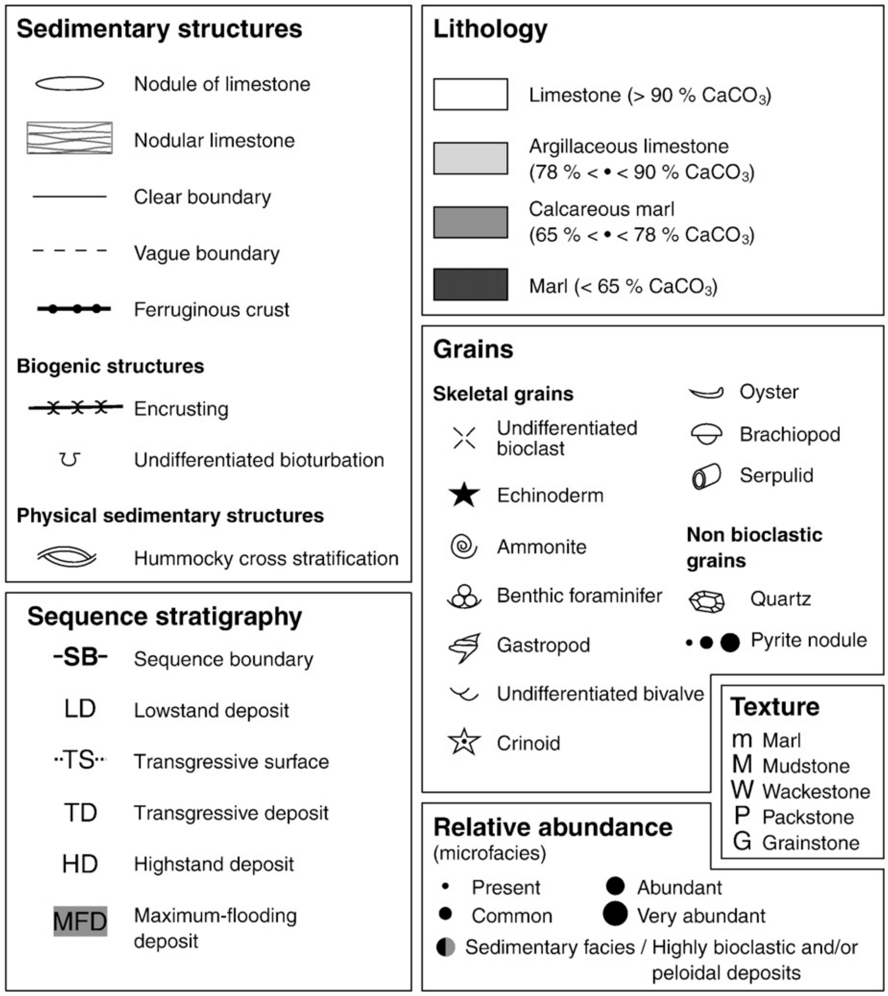

Fig. 4. Key for the Pas and Rocher d'Yves sections. Three pyrite nodule sizes are distinguished: small (less than 1 mm), medium (between 1 mm and 1 cm), and large (more than 1 cm).

include marl–limestone alternations, but the Pas section is more calcareous than the Rocher d'Yves section. The Pas section corresponds to marls and argillaceous limestones that indicate external platform depositional environments (Hantzpergue, 1988). Coral reefs occur at the end of the Early Kimmeridgian (Olivier et al., 2003, 2008), around 10 m above the Pas section, after discontinuity D3 (Fig. 2), along Hercynian faults (Fig. 1). These reefs indicate more proximal environments than previously. They disappear during the Late Kimmeridgian, and are replaced by the "virgulian" facies, which uniformly covers the entire La Rochelle platform (Hantzpergue, 1988).

3. Material and methods

A detailed bed-by-bed log was made for each section, containing field observations, thicknesses, lithologies, samples, textures, allochem contents and sedimentary structures. The key is shown in Fig. 4. Forty samples, representing the different lithologies and sedimentary structures observed in the field, were selected for microfacies analyses. Calcimetry was done to specify lithology defined in the field, by measuring CO_2 emissions under exposure to hydrochloric acid. Marls correspond to 35 to 65% $CaCO_3$, calcareous marls comprise between 65 and 78% $CaCO_3$, argillaceous limestones between 78 and 90% $CaCO_3$, and limestones have values higher than 90%. The relative abundances of allochems were estimated by counting them under a light microscope. Allochems in sedimentary facies were counted at 40× magnification, except for quartz and pyrite, which are smaller than the other allochems, and were counted at 100× magnification. The two sections also exhibit bioclastic and/or peloidal deposits containing sedimentary structures. In these, allochems were systematically counted at 100× magnification. All of these observations allow the definition of sedimentary facies and their interpretation as depositional environments. Also the bioclastic and/or peloidal deposits observed in the field and in thin section were thus characterised and interpreted.

<table>
<tr><th>Origin</th><th colspan="2">Group</th><th>Constituent</th><th>Types</th><th>Composition (maceral)</th></tr>
<tr><td rowspan="7">Continental</td><td rowspan="5">Higher plant debris</td><td rowspan="5">Phytoclasts</td><td>semi-opaque</td><td>PM1</td><td rowspan="2">Vitrinite</td></tr>
<tr><td rowspan="2">translucent</td><td>PM2</td></tr>
<tr><td>PM3</td><td>Cutinite</td></tr>
<tr><td rowspan="2">opaque</td><td>PM4E (equi.)</td><td rowspan="2">Inertinite</td></tr>
<tr><td>PM4T (blade)</td></tr>
<tr><td rowspan="2">Sporomorphs</td><td rowspan="9">Palynomorphs</td><td colspan="2">Spores</td><td rowspan="9">Exinite</td></tr>
<tr><td colspan="2">Pollens</td></tr>
<tr><td rowspan="7">Marine</td><td rowspan="6">Marine phytoplankton</td><td rowspan="4">Dinocysts</td><td>proximates</td></tr>
<tr><td>proximochorates</td></tr>
<tr><td>chorates</td></tr>
<tr><td>cavates</td></tr>
<tr><td colspan="2">Acritarchs</td></tr>
<tr><td colspan="2">Other marine algae</td></tr>
<tr><td>Foraminifera</td><td colspan="2">Foraminifera test linings</td></tr>
</table>

Fig. 5. Palynofacies constituents used in this study, modified from Steffen and Gorin (1993) and Courtinat et al. (2003) (equi. = equidimensional, blade = blade-shaped).

Palynofacies constituents are the organic particles used to describe palynofacies (Fig. 5, modified from Steffen and Gorin, 1993, and Courtinat et al., 2003). Sixty-four samples were selected for palynofacies analyses with a sampling resolution of 1 to 1.5 m. The samples reflect all of the encountered lithologies. Palynofacies slides were made according to the standard palynological preparation method (e.g. Steffen and Gorin, 1993). In order to avoid any statistical skew, at least 300 particles were counted at 250× magnification for each slide (Courtinat et al., 2003).

Seventy-eight samples, corresponding to different lithologies, were selected for calcareous nannofossil analyses. Smear-slides were created following the method of Geisen et al. (1999), which

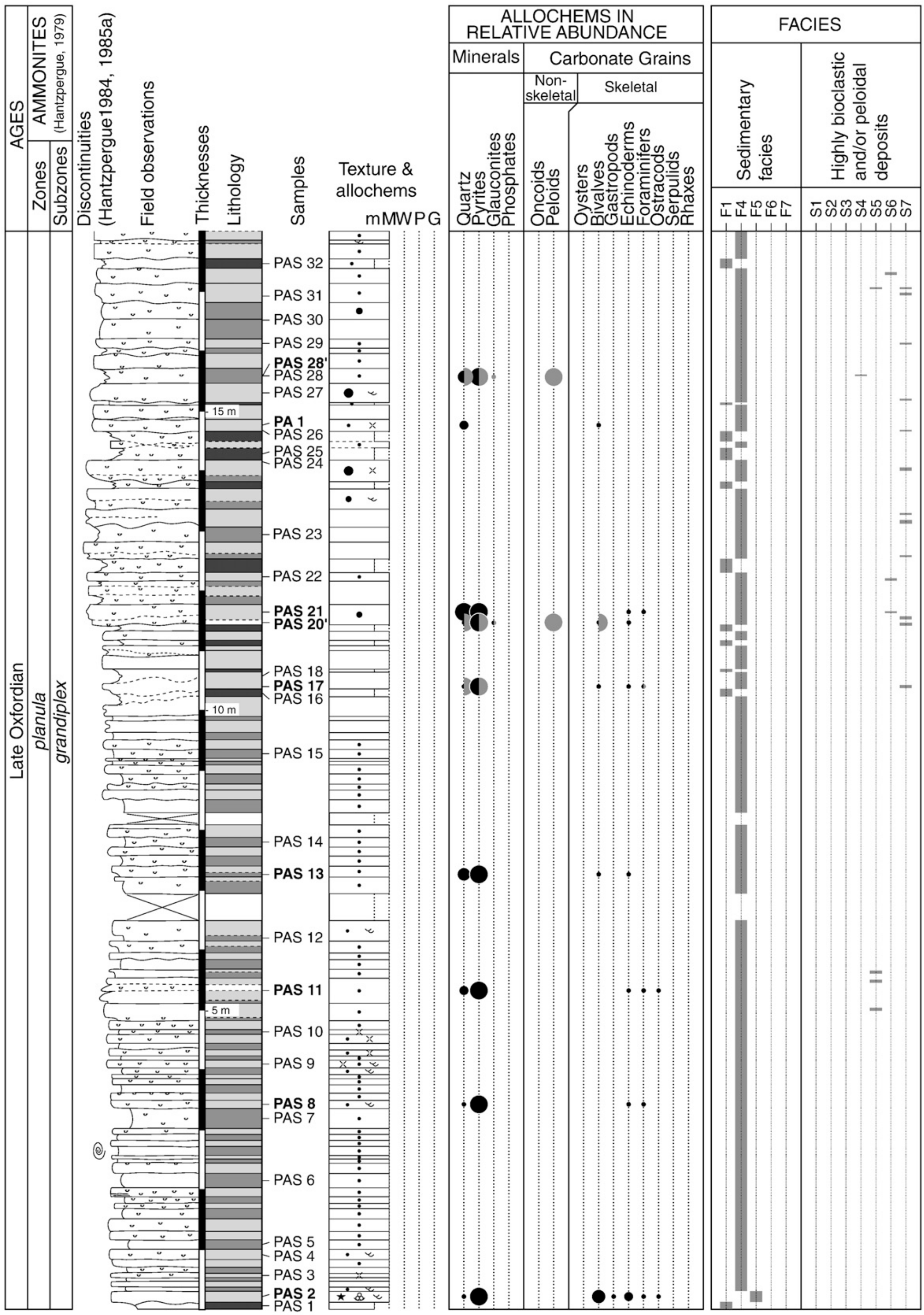

Fig. 6. Facies and microfacies details in the Pas section.

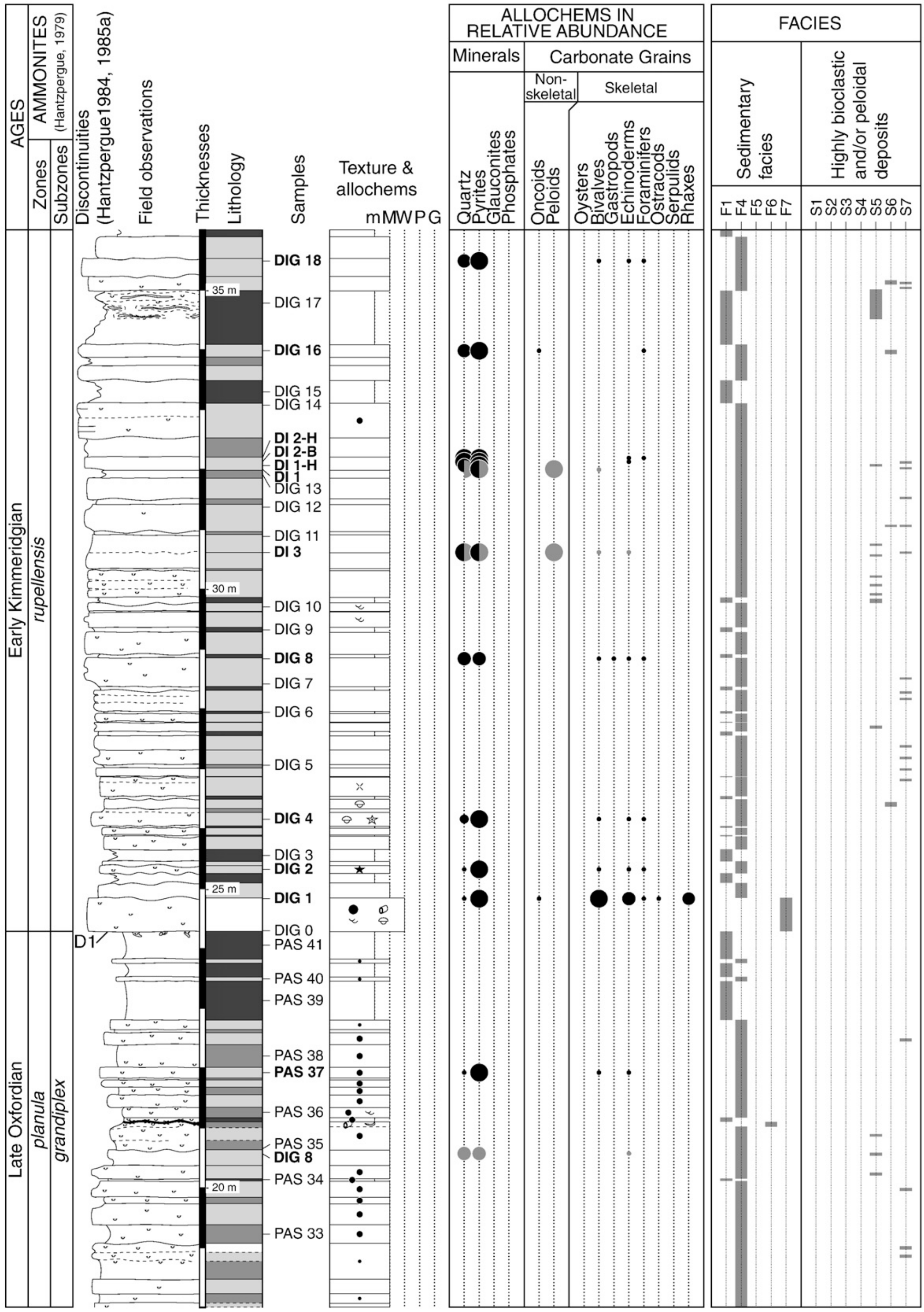

Fig. 6 (*continued*).

allows the calculation of the absolute abundance of calcareous nannofossils. Three types of calcareous nannofossils were identified: ascidian spicules, coccoliths, and schizospheres (see Appendix for a taxonomic list). For coccoliths and schizospheres, 300 specimens were generally counted in each smear-slide under a polarising microscope at 1560× magnification. In samples with rare nannofossils, specimens were counted following a transverse (200 fields of view) on smear-slides. Ascidian spicules were counted separately because of their very high abundance with respect to other nannofossils. In order to better describe the coccolith assemblages,

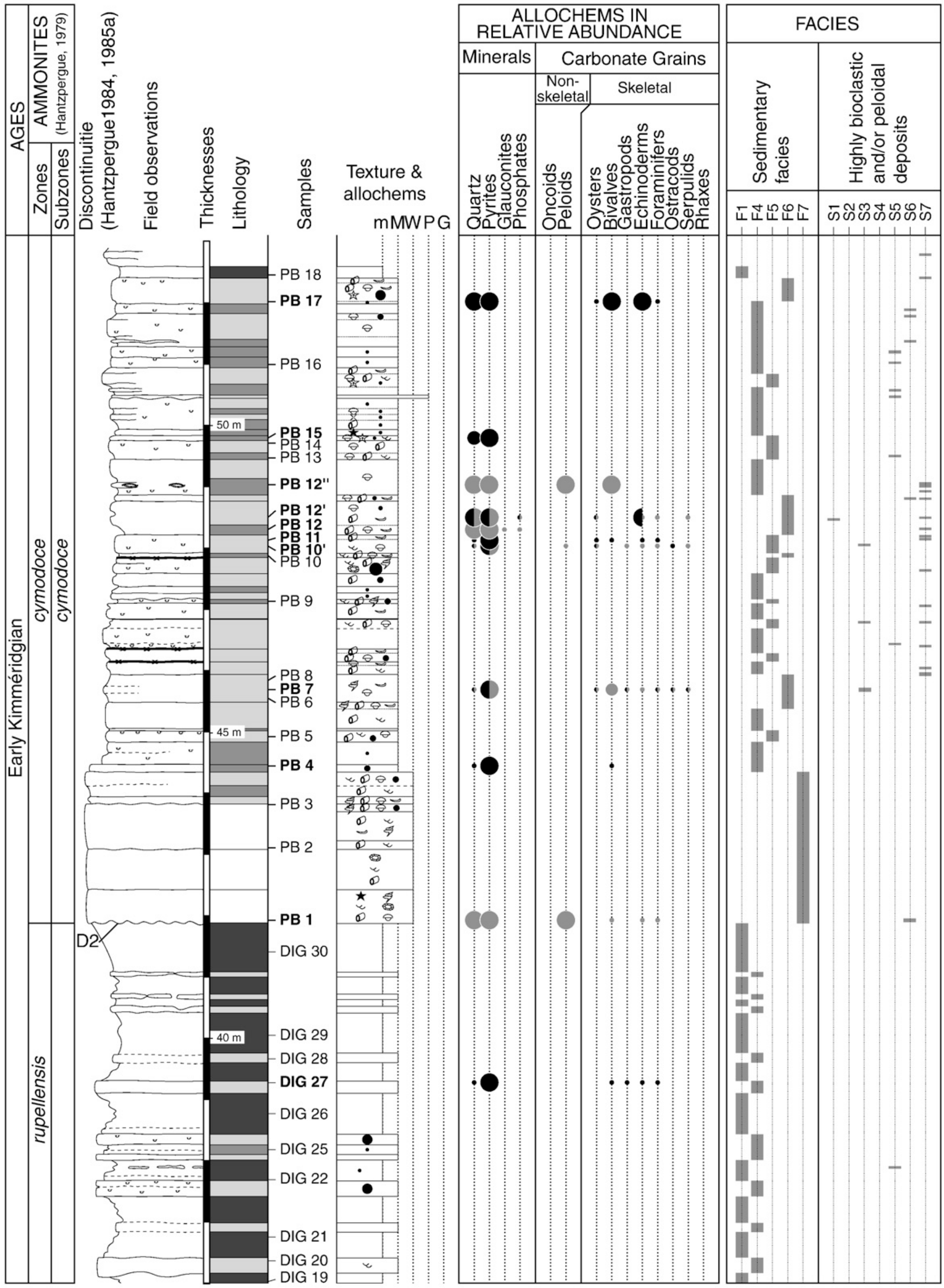

Fig. 6 (*continued*).

diversity, measured by the Shannon index (1), and evenness (2), were calculated and compared with species richness.

$$H = -\sum_{i=1}^{S} p_i \ln p_i \qquad (1)$$

$$E_H = H / \ln S. \qquad (2)$$

H: Shannon index, E_H: evenness, S: species richness, and p_i: relative abundance of each species.

Sedimentary facies and palynofacies analyses allow the definition of depositional sequences that reflect variations in relative sea level. Sequences were defined according to Strasser et al. (1999). Elementary sequences are the smallest units observable in the repetitive stackings of beds. These elementary sequences form small-scale sequences, which themselves stack into medium-scale sequences, which form large-scale sequences. Small-, medium-, and large-scale sequences thus defined are similar to those of Vail (1987). However, the outcrops do not allow the observation of the geometries of system tracts (Vail et al., 1991). Consequently, instead of lowstand, transgressive, and highstand system tracts, the terms lowstand, transgressive, and highstand deposits are used. A cyclostratigraphic interpretation is proposed according to the stacking pattern of the different orders of sequences and the durations of the ammonite zones.

4. Results

4.1. Sedimentology

4.1.1. Section description

The Pas section presents beige to light-grey marl–limestone alternations (Fig. 6). The lower part of this section corresponds to 22 m of calcareous marl–argillaceous limestone alternations with some marl–argillaceous limestone alternations between metres 10 and 15. This lower part ends with 2 m of marl–argillaceous limestone alternations, largely dominated by marls. The top of this interval corresponds to a sharp erosional surface, located between the most marly interval and a massive, bioturbated wackestone bed. Above this bed, the middle of the section is composed of 14 m of mainly marl–argillaceous limestone alternations. These alternations are covered by another 3 m marly interval with thin argillaceous limestone beds, which is also capped by a sharp erosional surface. This surface is followed by three red–brown, massive, and bioturbated wackestone beds, in turn followed by 9 m of calcareous marl–argillaceous limestone alternations, which form the upper part of the section. Calcareous beds are thicker than marly beds in this interval. The two erosional surfaces are located at the boundaries between the *planula* and the *rupellensis* ammonite Zones, and between the *rupellensis* and *cymodoce* Zones, respectively. They correspond to the D1 and D2 discontinuities identified by Hantzpergue (1984, 1985a). The D1 discontinuity also corresponds to the boundary between the Oxfordian and Kimmeridgian stages.

The Rocher d'Yves section is composed of dark-grey marl–argillaceous limestone alternations that present a high abundance of *N. virgula* oysters (Fig. 7). The section starts with a 1 m-thick marly interval that contains abundant lenses and layers of *N. virgula* packstones. It is followed by three massive mudstone beds with *N. virgula* packstone lenses. The upper part of the section is composed of 7 m of marl–argillaceous limestone alternations, and ends with 1 m of *N. virgula* marls. In the last 3 m of marl–argillaceous limestone alternations, only subtle variations in induration and coloration allow the differentiation between calcareous beds and marly beds.

4.1.2. Facies description

Seven facies are defined according to the texture, which is mudstone (Fig. 8a) or wackestone (Fig. 8b), the lithology, and the most abundant allochems (Fig. 9). The contents in allochems of argillaceous limestones and calcareous marls are the same. Thus, these two lithologies were associated in the definition of facies F3 to

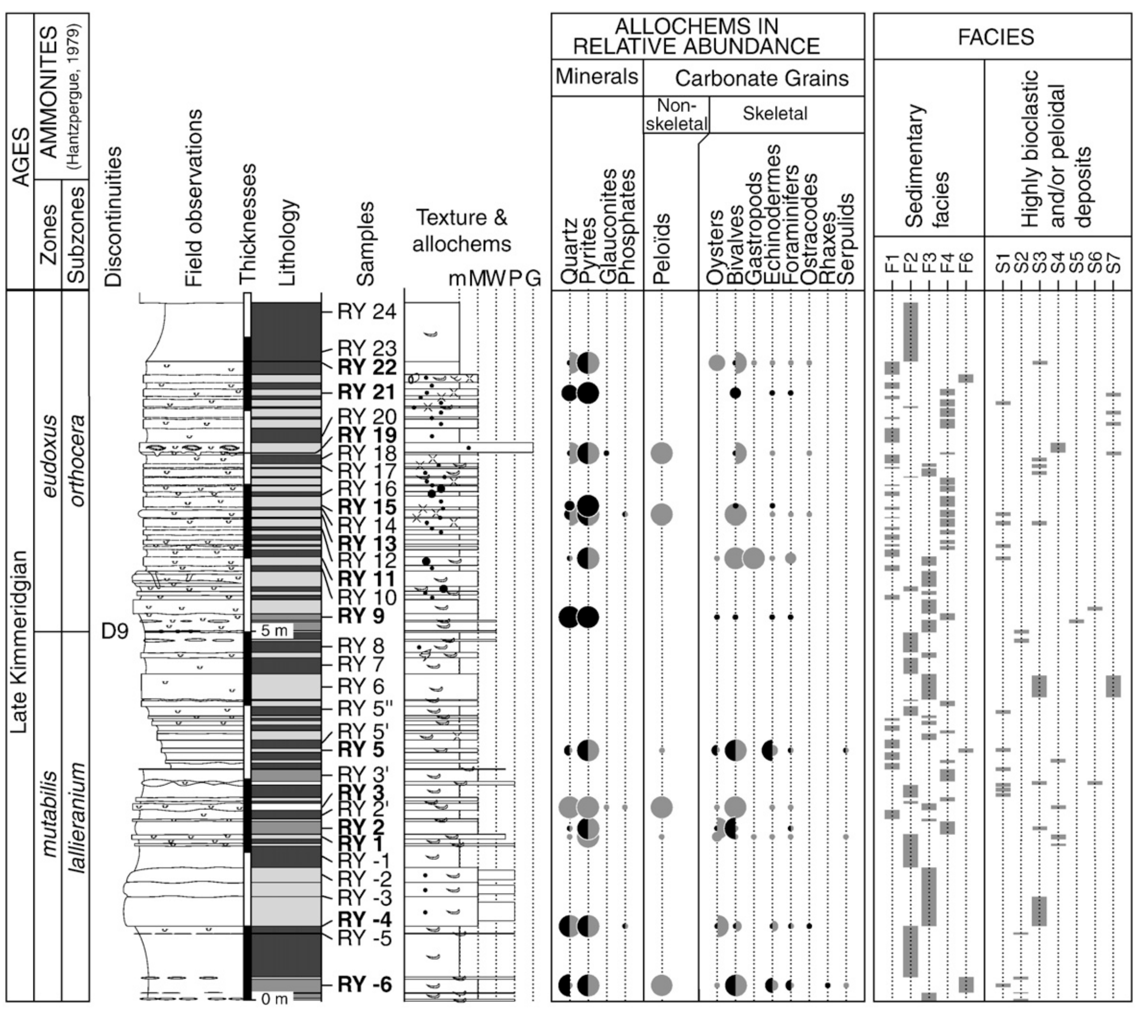

Fig. 7. Facies and microfacies details in the Rocher d'Yves section.

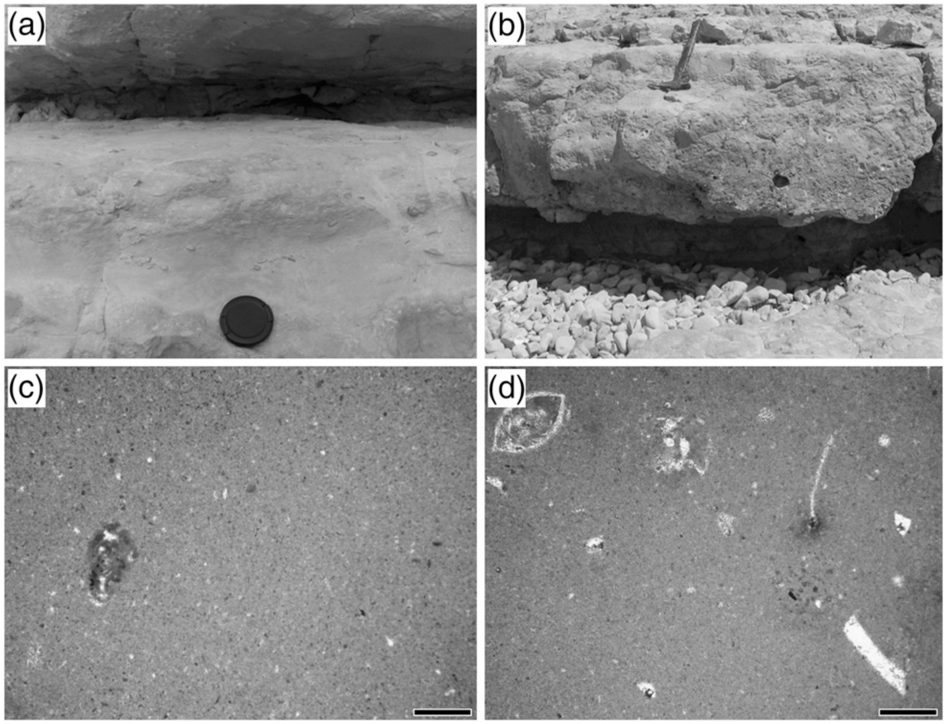

Fig. 8. Pictures of different sedimentary facies. (a) and (b) are macroscopic pictures of facies F6 and F7, respectively. (c) and (d) are microscopic pictures taken in natural light of facies F4 and F5, respectively. Scale represents 0.4 mm.

F6 (Fig. 9). Bioclast abundance and diversity, and calcium carbonate contents are the main features that allow the definition of these facies. These parameters globally increase from facies F1 to F7 (Fig. 9), as revealed by thin sections (Fig. 8c and d).

The lower and the middle parts of the Pas section consist of alternations between facies F1 and F4 (Fig. 6). Only one occurrence of facies F6 is observed at the end of the *planula* Zone. Facies F5 and F6 are present in the upper part of the Pas section. Facies F7 occurs twice, capping the two erosional surfaces present in the Pas section (Fig. 6). The Rocher d'Yves section exhibits facies F1 to F4 and facies F6.

4.1.3. Highly bioclastic and/or peloidal deposits

Seven types of highly bioclastic and/or peloidal deposits (S1 to S7) are defined for the two sections, according to the size of the allochems they contain and their shapes (Fig. 10). These deposits are mainly present in facies F2 to F6, and are largely concentrated in facies F4, which is the most common facies in the two sections (Figs. 6 and 7). These deposits are a few millimetres to a few centimetres thick. They present sharp and erosive bases (Fig. 11a, b, g and i), except for S3 and S6 (coarse and fine patches, respectively), which present more diffuse bases (Fig. 11e). Horizontal preferential orientation of both convex-up and convex-down shells (Fig. 11d and e) is a common feature of these deposits. Normal grading (Fig. 11f and h) is not systematically present. Cross (Fig. 11g, i and j) and planar (Fig. 11f) laminations are only present in fine deposits and laminae (S4 to S7).

Allochems within the highly bioclastic and/or peloidal deposits are micrite- (Fig. 11a) or both micrite- and sparite-supported (Figs. 11b and d). The texture is wacke-packstone or wacke-pack-

Facies	Texture - Lithology	Main components (from the most to the least abundant)
F1	M - marl	
F2	M - marl	Oysters
F3	M -calcareous marl / argillaceous limestone	Oysters
F4	M - calcareous marl / argillaceous limestone	Relatively low abundance and diversity of bioclasts (undifferentiated bivalves and bioclasts)
F5	M - calcareous marl / argillaceous limestone	Relatively high abundance and diversity of bioclasts (echinoderms, undifferentiated bivalves, and foraminifers)
F6	M - calcareous marl / argillaceous limestone	Relatively high abundance and diversity of bioclasts (echinoderms, undifferentiated bivalves, and foraminifers) and oysters
F7	W - limestone	High abundance and diversity of bioclasts (echinnoderms, undifferentiated bivalves, foraminifers, brachiopods, and serpulids)

Fig. 9. Facies defined in the Pas and Rocher d'Yves sections. These are reported on the Pas and Rocher d'Yves sections, respectively, in Figs. 6 and 7.

Deposits	Granulometry and shape	Type of base	Texture	Main allochems (from the most to the least abundant)
S1	Coarse (millimetric) bioclastic layer	Sharp erosional	W-P-G	Undifferentiated bivalves, oysters, peloïds
S2	Coarse (millimetric) bioclastic lens	Sharp erosional	W-P-G	
S3	Coarse (millimetric) bioclastic patch	Diffuse	W	
S4	Fine (around 100 µm) layer	Sharp erosional	W-P-G	Quartz, peloids, undifferentiated bivalves
S5	Fine (around 100 µm) lens	Sharp erosional	W-P-G	
S6	Fine (around 100 µm) patch	Diffuse	W	
S7	Laminae (5 to 50 µm)	Sharp erosional	W-P-G	

Fig. 10. Highly bioclastic and/or peloidal deposits observed in the Pas and Rocher d'Yves sections. These are reported on the Pas and Rocher d'Yves sections, respectively, in Figs. 6 and 7.

grainstone, except for coarse and fine patches (structures S3 and S6, respectively), which are wackestones. The Pas section preferentially contains fine deposits and laminae (S4 to S7), while the Rocher d'Yves section presents a high proportion of coarse deposits (S1 to S3). In the two sections, some deposits contain allochems that are not present in the rest of the samples (Figs. 6 and 7): for instance, samples Di 1, Di 3, PB 7, PB 10′, and PB 12 in the Pas section and RY-4, RY 2, RY 5 and RY 22 in the Rocher d'Yves section. The tops of the highly bioclastic and/or peloidal deposits are commonly strongly bioturbated (Fig. 11c and h).

4.2. Palynofacies

Palynofacies observed in the Pas (Fig. 12) and Rocher d'Yves (Fig. 13) sections are mainly composed of woody fragments and dinocysts, with an average of 77% and 10%, respectively. Small quantities of spores, pollen, marine algae other than dinoflagellates (mainly tasmanids), and foraminifera linings are also present. Palynomorphs are more abundant in the Rocher d'Yves section than in the Pas section, with an accumulated maximum of about 10%. Dinocysts, which dominate the palynomorphs in both sections, are very sensitive to degradation, and thus are good indicators of general organic-matter preservation (Bombardiere and Gorin, 1998). The Pas section presents a lot of fragmented and poorly preserved dinocysts. Dinocysts are well preserved in the Rocher d'Yves section, indicating a better preservation of the organic matter than in the Pas section.

$CaCO_3$ is relatively constant in the Pas section (Fig. 12), with an average value of 74%, except for higher values in the wackestone beds (metres 25 and 43). The amorphous organic matter (AOM) is well represented in both sections, with an average value of 12.5%. The AOM signal of the Pas section is relatively constant (Fig. 12), but percentages are slightly higher in the *planula* Zone than in the *rupellensis* and *cymodoce* Zones (14.5% and 11%, respectively), and two peaks around 50% are observed in the wackestone beds (Fig. 12). The Pas section shows an increase in the marine/continental ratio in its lower part, followed by a strong decrease (more than 25%) at the end of the *planula* Zone. Values of the marine/continental ratio stay low (less than 10%) in the middle and upper parts of the Pas section (Fig. 12). The opaque/translucent ratio does not show any particular trend, except in the massive wackestone beds (facies F7, metres 25 and 43), while it strongly decreases (Fig. 12) due to a high amount of very degraded, brown to translucent woody particles. The PM4T/PM4E ratio progressively decreases throughout the *planula* and *rupellensis* Zones, from 19% at the base of the section to 4% at the end of the *rupellensis* Zone (metre 40), and increases at the end of the *rupellensis* Zone and in the first half of the *cymodoce* Zone.

$CaCO_3$ fluctuates from 48 to 97% (average value of 63%) in the Rocher d'Yves section, with a very low value (28%) at the top of the section (Fig. 13). The AOM content in the Rocher d'Yves section is lower (average value of 7%) than in the Pas section (Figs. 12 and 13). The marine/continental ratio presents overall higher fluctuations in the Rocher d'Yves section than in the Pas section. The average ratio shows a small decrease from the base (30%) to the top (20%) of the section. The opaque/translucent and PM4T/PM4E ratios globally follow opposite trends. The relative abundance of AOM correlates positively with the calcium carbonate content in the Pas section ($r = 0.5783/p = 0.0001$), but there is no correlation observed in the Rocher d'Yves section ($r = 0.1607/p = 0.4533$).

4.3. Calcareous nannofossils

Three types of calcareous nannofossils are observed in the samples of the Pas section: coccoliths, schizospheres and ascidian spicules. Coccolith preservation varies from bad to good (Fig. 14). The absolute abundance of ascidian spicules is relatively constant (average value of $1.5*10^{10}$ spicules per gram of rock), excepting a sharp decrease at the base of the *cymodoce* Zone (Fig. 14). The absolute abundance of coccoliths and schizospheres is also relatively constant (average value of $1.6*10^{7}$ per gram of rock) in the lower part of the Pas section, before a first decrease at the top of the *planula* Zone (Fig. 14). The fluctuation of the absolute abundance of coccoliths and schizospheres in the middle part of the Pas section is more important, and a second strong decrease is recorded at the base of the *cymodoce* Zone. The absolute abundances of ascidian spicules, coccoliths and schizospheres present very low values in the second interval of massive wackestone beds (Fig. 14, metre 43), except for one point at the base of the third bed. Species richness and diversity of coccoliths are low in the Pas section, and follow the same trend as the absolute abundances, with a maximum in diversity and species richness in the upper part of the *rupellensis* Zone. Evenness shows lower values in the first half of the *rupellensis* Zone than in the rest of the section.

The calcareous nannofossil assemblages of the Pas section (Fig. 14) are dominated by *Watznaueria* spp. (average value of 56%, maximum value of 90%). *Watznaueria britannica* is the most abundant species (average value of 41%, maximum value of 63%). The six morphotypes of *W. britannica*, described by Giraud et al. (2006) in the Late Jurassic of the western Swabian Alb (southern Germany), are recognised in the Pas section. *Cyclagelosphaera margerelii* also presents a high relative abundance (average value of 27%, maximum value of 67%). *Watznaueria barnesiae*, *W. fossacincta*, *W. biporta* and *Schizospherella* spp. are common (Fig. 14). *Watznaueria barnesiae* and *W. fossacincta* were lumped together because they are believed to represent end-members of a morphological continuum (Lees et al., 2004, 2006; Bornemann and Mutterlose, 2006). *Lotharingius hauffii* is rare to abundant.

Watznaueria britannica dominates the assemblages of the *planula* Zone, and then its relative abundance decreases until the second erosional surface, which corresponds to the end of the *rupellensis* Zone (Fig. 14). *Lotharingius hauffii* is present at the base of the section (Fig. 14). It presents higher relative abundances than previously

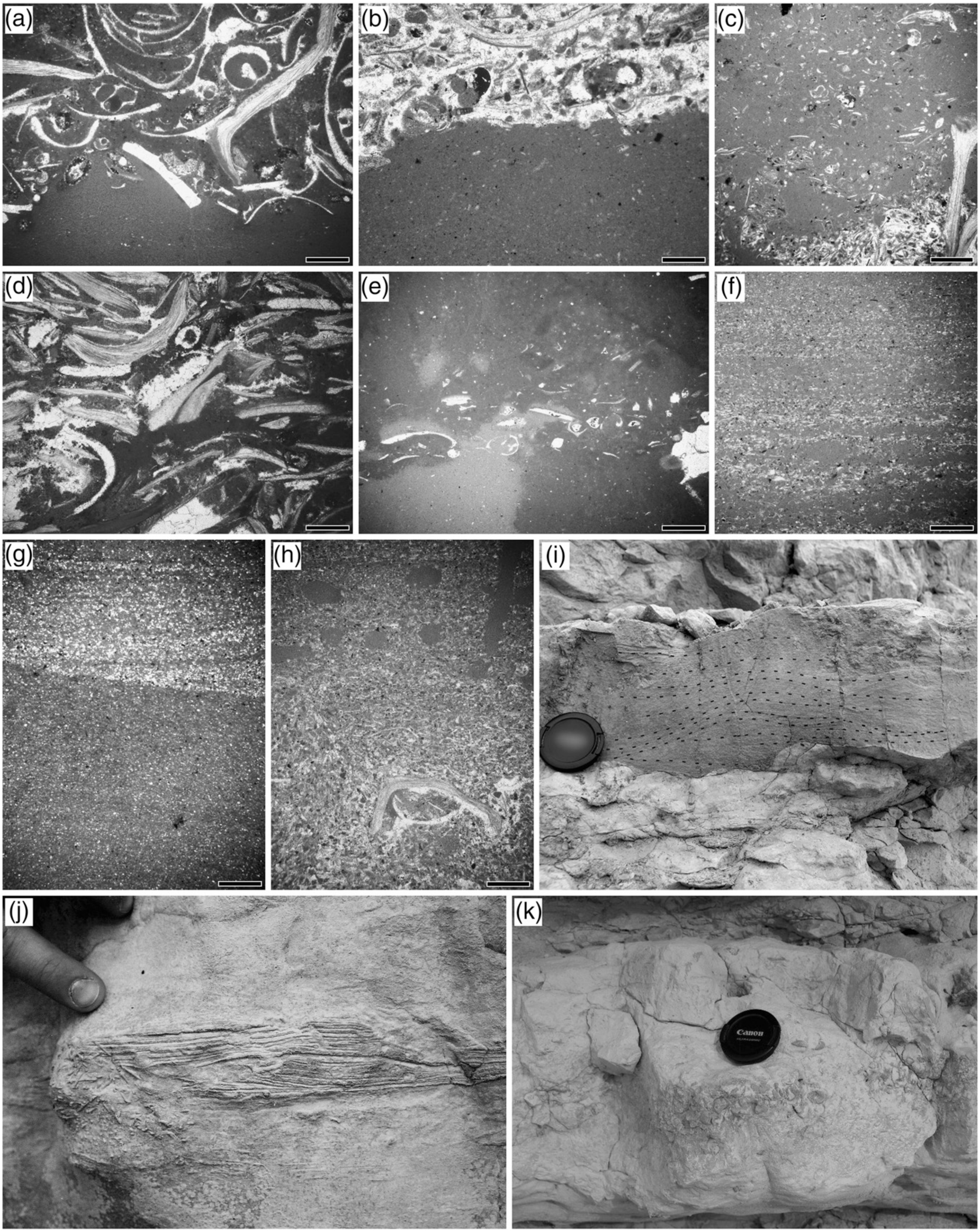

Fig. 11. Pictures of the different bioclastic and/or peloidal deposits observed under a light microscope (a to h) and macroscopically (i to k). Scale represents 1 mm, except for picture h which is 0.4 mm. All microscopic pictures are taken in natural light. (a) Coarse wacke-packstone (structure S1) with sharp base on facies F3. (b) Coarse wacke-grainstone (structure S1) with sharp base on facies F3. (c) Coarse bioturbated top of a structure S1, with pack-grainstone texture at the base, becoming wackestone at the top. (d) Coarse wacke-grainstone with oriented bioclasts (structure S1). (e) Coarse bioclastic wackestone (structure S3) with diffuse base on facies F3. (f) Finely laminated wacke-packstone (structure S4). (g) Fine, cross-stratified wacke-packstone with sharp base (structure S7). (h) Fine wacke-packstone (structure S4), normally graded and bioturbated at the top. (i) Fine bioclastic layer with hummocky cross-stratification and sharp erosive base (structure S4). (j) Finely cross-stratified laminae (structure S7). (k) Coarse bioclastic patch (structure S3).

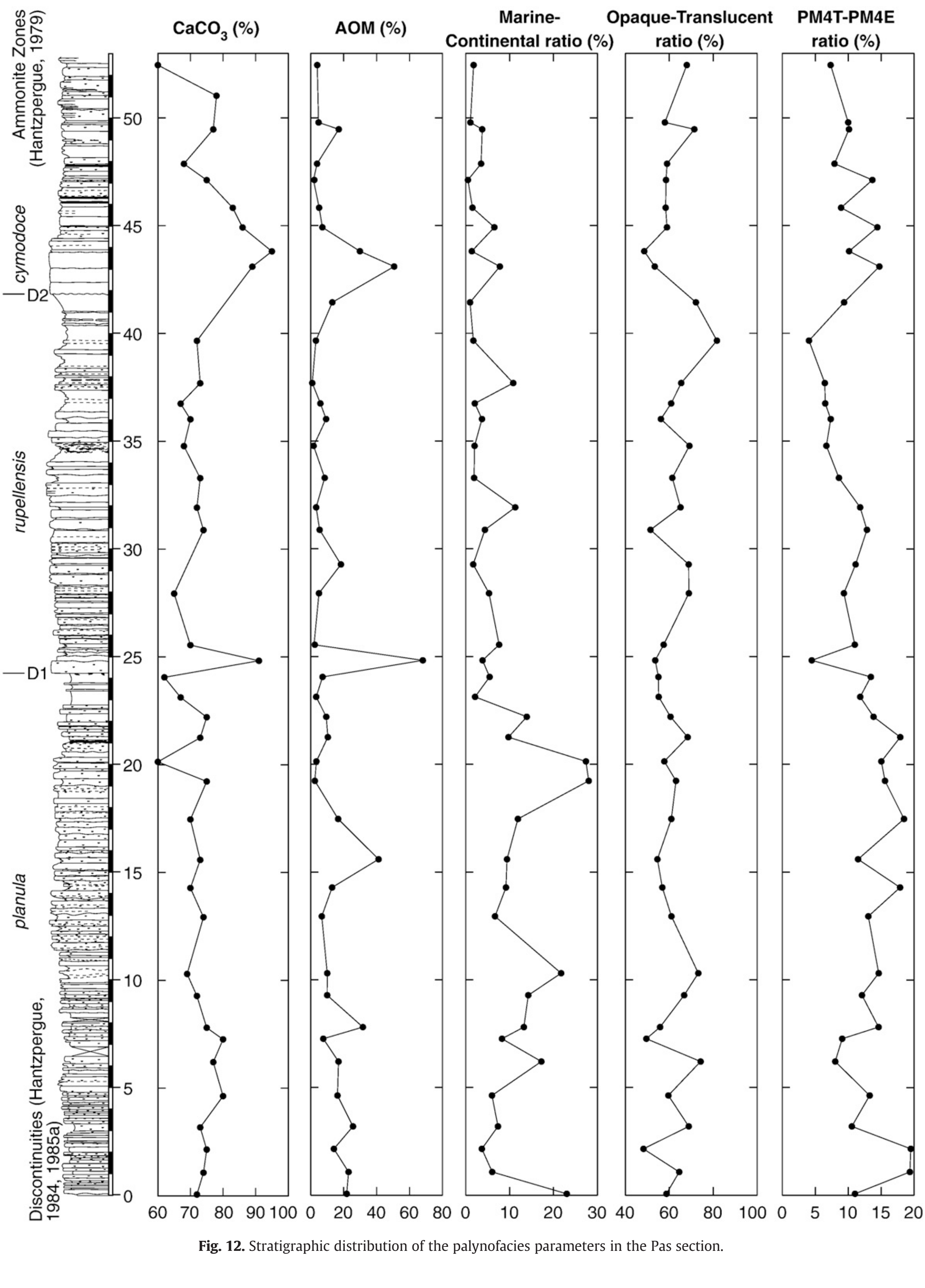

Fig. 12. Stratigraphic distribution of the palynofacies parameters in the Pas section.

around the boundary between the *planula* and *ruppelensis* Zones (Fig. 14). *Schizosphaerella* spp. is frequent after metre 27, and reaches its maximum in relative abundance (31%) at the end of the *rupellensis* Zone (Fig. 14). The upper part of the Pas section is characterised by a dominance of small coccoliths in the nannofossil assemblages. *Watznaueria britannica* is the most abundant taxon (average value of 42%), with a dominance of small specimens (morphotype A). *Cyclagelosphaera margerelii* (average value of 18%) and *L. hauffii* (average value of 5%) are abundant.

Only ascidian spicules and coccoliths are observed in the Rocher d'Yves section (Fig. 15). The preservation of coccoliths is moderate to good. Some samples are barren or present only rare coccoliths. The absolute abundance of ascidian spicules strongly fluctuates, with an average value of 10 billion per gram of rock. The absolute abundance of coccoliths presents a peak (more than 300 billion) at the base of the section (Fig. 15), followed by relatively low values (average value of $7*10^6$ per gram of rock). Because of the quasi-monospecific assemblages of *C. margerelii* observed in the Rocher d'Yves section

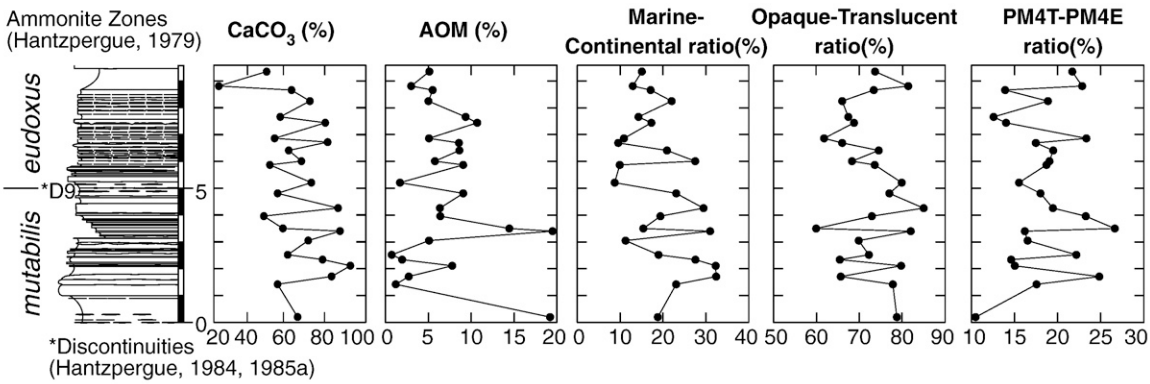

Fig. 13. Stratigraphic distribution of the palynofacies parameters in the Rocher d'Yves section.

(see description in the next paragraph), the species richness, diversity, evenness, and relative abundances are not plotted (Fig. 15). *Watznaueria britannica* (morphotypes A and B) is also present (maximum value of 5%).

In the two sections, *Cyclagelosphaera* spp. are generally more affected by dissolution or recrystallisation than other species, and larger coccoliths are generally more poorly preserved than smaller ones. In the two sections, the absolute abundance of ascidian spicules is higher than those of both coccoliths and schizospheres. The absolute abundances of ascidian spicules, coccoliths, and schizospheres are negatively correlated with calcium carbonate content, and the absolute abundances of ascidian spicules and coccoliths are positively correlated in the Pas section (Table 1). No correlations are observed in the Rocher d'Yves section (Table 2).

5. Interpretation

5.1. Facies models

5.1.1. Vertical facies succession

The Pas and Rocher d'Yves sections correspond to a mixed carbonate-siliciclastic platform. Most macro- and micro-fossils observed in the field and in thin sections are ubiquitous organisms. However, undifferentiated echinoderm fragments, oysters, undifferentiated bivalves, and benthic agglutinated foraminifera (suborder Textulariina) dominate the fossil associations, and indicate shallow- and normal-marine depositional environments (Tucker and Wright, 1990; Flügel, 2004). Mudstones are dominant and indicate low-energy depositional environments. Clays came from land and form more argillaceous deposits. Clay can float over long distances, and form deep-sea deposits. However, sedimentary facies variations are weak, suggesting few relative sea-level variations. Consequently, these argillaceous deposits could be formed along the coast line, and consequently are more proximal than calcareous deposits.

Moreover, an increase in the abundance and diversity of the bioclastic content is also observed from the most proximal to the most distal environments. However, an exception is observed. According to its high carbonate and bioclastic contents, F7 should be the most distal facies. However, its position is hard to define on the proximal–distal transect, and in addition it appears sparsely (only two occurrences in a 63 m section). The significance of this facies is discussed later (see Sections 5.2 and 5.4).

The facies evolution reflects the spatial organisation on a proximal–distal transect. Fig. 16 shows an example of the most complete small-scale sequences observed in the Pas and Rocher d'Yves sections. In the Pas section, alternations between F1 and F4 are observed all along the lower and the middle parts of the section (Fig. 6). In the upper part of the Pas section, transitions from F4 to F5 and from F5 to F6 are common, and succession F4 to F5 to F6 is observed at metre 48 (Fig. 6). As sedimentary facies become more bioclastic as they are more distal, and as F6 is more bioclastic than F5, which is more bioclastic than F4, the facies succession F4 to F5 to F6 indicates a deepening tendency. A similar vertical succession, from F2 to F3 to F4, is also observed in the Rocher d'Yves section (Fig. 16). These vertical successions suggest a horizontal organisation of the sedimentary facies, from F1 in the most proximal settings to F6 in the most distal settings.

Oyter-rich facies F2 and F3 are only present in the Rocher d'Yves section. They are largely dominated by *N. virgula*. This oyster is known to live on hardgrounds as well as on soft sediment (Fürsich and Oschmann, 1986). Today, oysters preferentially live in proximal environments, close to the coast line. This suggests that F2 and F3 are proximal sedimentary facies, which is in accordance with the proposed horizontal organisation of the sedimentary facies (Fig. 16).

5.1.2. Significance of the highly bioclastic and/or peloidal deposits

The observed highly bioclastic and/or peloidal deposits present a sharp and erosional base. They commonly develop as wacke-packstones or wacke-pack-grainstones. Allochems are horizontally oriented. They are well sorted if they are coarse (i.e., bioclasts that are recognisable with the naked eye), and the deposits present cross- or parallel-stratification if the grains are fine (i.e., bioclasts that are not recognisable macroscopically). These characteristics indicate high-energy deposits (Tucker and Wright, 1990; Flügel, 2004), and the combination of a sharp erosive base and a well-sorted organisation is characteristic of event deposits (Einsele et al., 1991, 1996). On a shallow platform, storms are the most likely phenomenon to have caused such high-energy structures (Aigner, 1982).

The tops of storm deposits are often reworked by bioturbation. This indicates a break in storm activity (Einsele et al., 1996; Flügel, 2004). The coarse and fine bioclastic patches (structures S3 and S6, respectively) contain allochems that are horizontally oriented, present a more diffuse but visible base (Fig. 11e), and sometimes a well-sorted organisation of the allochems can be observed. So they can be interpreted as storm deposits that are strongly reworked by bioturbation. This can result from lower-energy conditions, indicating less important storms or more distal parts of the storm deposits. In these cases, the storm deposits will be thinner and contain more mud (Flügel, 2004).

The allochem content of the storm deposits seems to be principally controlled by sedimentary facies: storm deposits of the Pas section, which contain very few coarse bioclasts, except in facies F7, are dominated by fine allochems (structures S4 to S7). Exceptions are localised in the upper part of the Pas section, in the *cymodoce* Zone, where the bioclastic content in the storm deposits becomes more diversified and coarser than in the lower part. The lower part of the Rocher d'Yves section contains coarser bioclasts, and storm deposits are also largely dominated by coarse allochems, which are fragmented

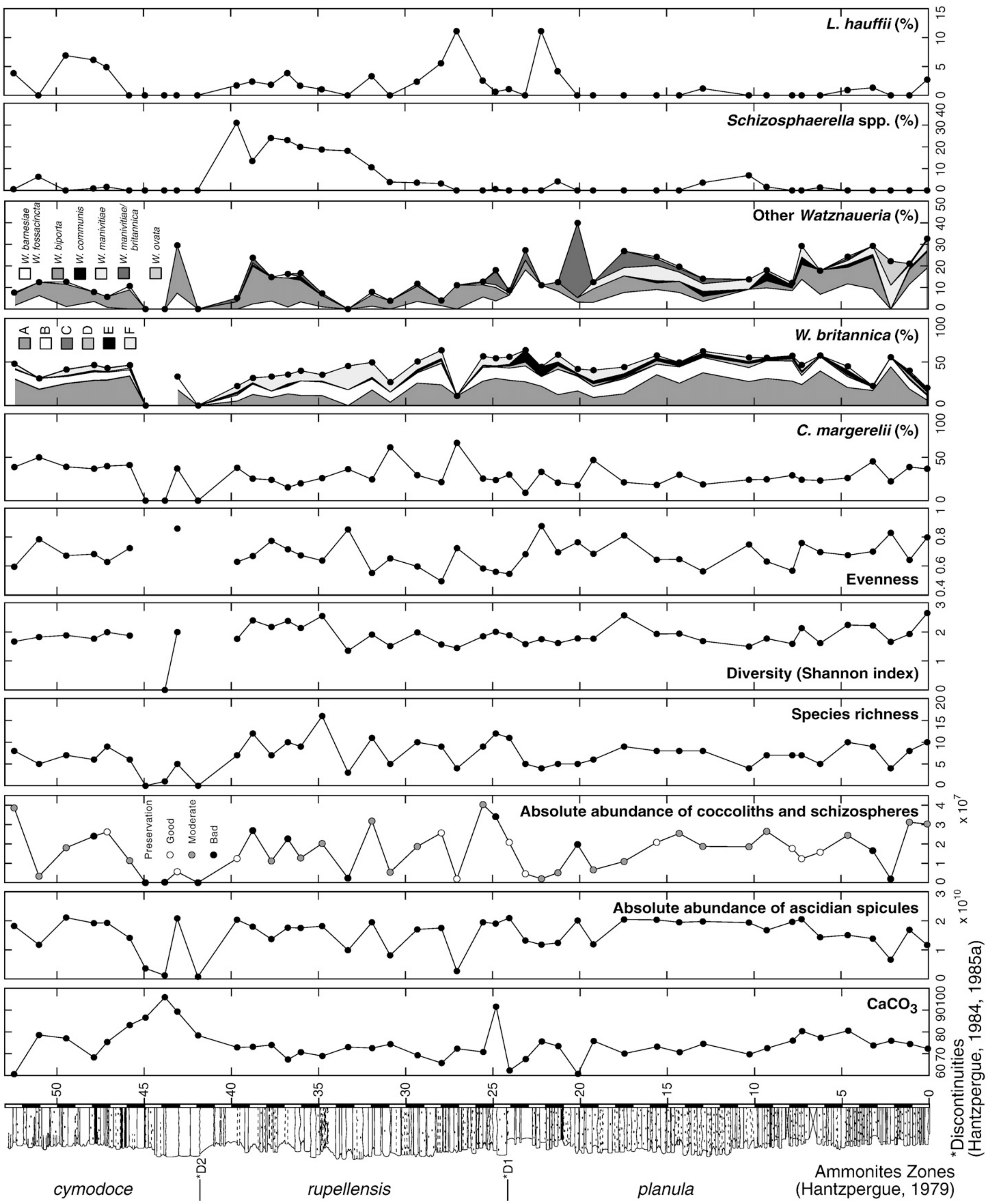

Fig. 14. Absolute abundances of calcareous nannofossils, species richness, and diversity, and relative abundances of selected taxa for the Pas section. A to F refer to the different morphotypes of *W. britannica*.

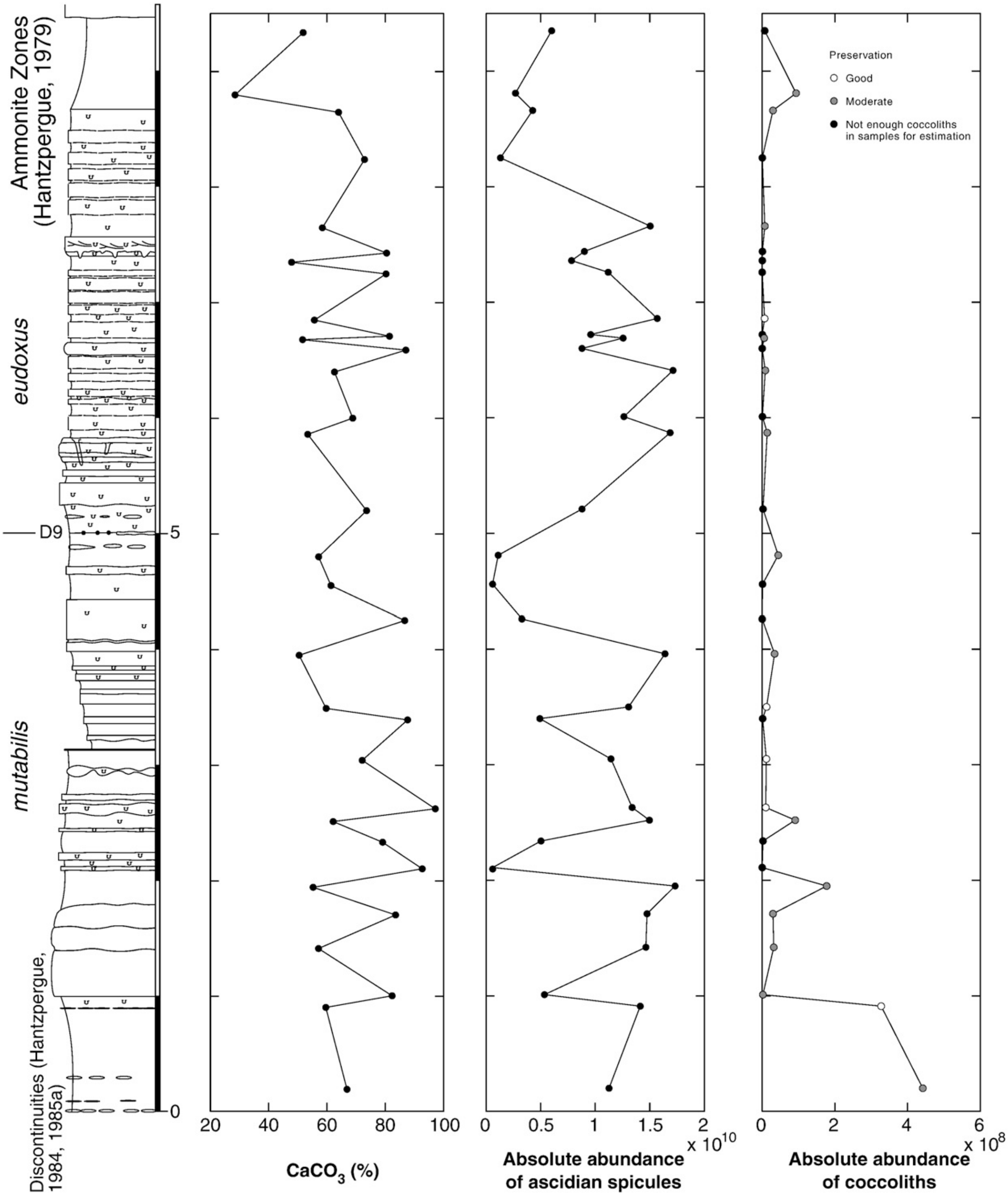

Fig. 15. Absolute abundances of calcareous nannofossils in the Rocher d'Yves section.

Table 1
Correlation indices between calcareous nannoplankton (coccoliths and schizospheres), ascidian spicules, and calcium carbonate content for the Pas section.

	$CaCO_3$	Calcareous nannoplankton	Ascidian spicules
$CaCO_3$	$r = 1.0000$		
Calcareous nannoplankton	$r = -0.3564$, $p = 0.0176$	$r = 1.0000$	
Ascidian spicules	$r = -0.3764$, $p = 0.0118$	$r = 0.6546$, $p < 0.0001$	$r = 1.0000$

Abbreviations: r: coefficient of correlation; p: probability.

Table 2
Correlation indices between calcareous nannoplankton (coccoliths), ascidian spicules, and calcium carbonate content for the Rocher d'Yves sections.

	$CaCO_3$	Calcareous nannoplankton	Ascidian spicules
$CaCO_3$	$r = 1.0000$		
Calcareous nannoplankton	$r = -0.2194$, $p = 0.2200$	$r = 1.0000$	
Ascidian spicules	$r = -0.2042$, $p = 0.2544$	$r = 0.1607$, $p = 0.4533$	$r = 1.0000$

Abbreviations: r: coefficient of correlation; p: probability.

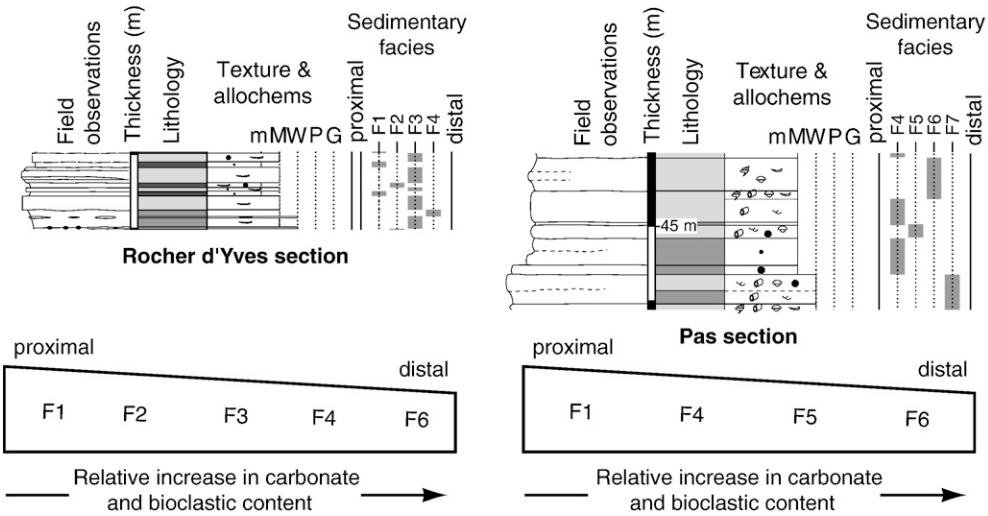

Fig. 16. Facies organisation proposed on a proximal–distal transect, according to the observed sedimentary features and vertical succession of facies. Vertical facies successions correspond to small-scale sequence 34 of the Pas section and small-scale sequence 5 of the Rocher d'Yves section.

oyster and undifferentiated bivalve shells (Fig. 7). However, allochems that are present in storm deposits are also present in smaller proportions in the rest of the sediments (see Figs. 6 and 7) or are not present at all. This can be explained by the transport of these allochems over a long distance by storm-induced currents (Gagan et al., 1988, 1990).

5.1.3. Contribution of the storm deposits to the facies model

The presence of storm deposits is a common feature of mid-ramp sediments (Burchette and Wright, 1992; Reading and Burchette, 1996). However, they are diluted in the Pas section, and more frequent in the Rocher d'Yves section. This could be the result of the more proximal conditions that prevailed in the Rocher d'Yves section, but also from an increase in storm activity. Moreover, storm deposits are relatively scarce compared to other shallow areas during the Kimmeridgian (for instance Iberia, Bádenas and Aurell, 2001b). This could be due to the emerged lands localised to the south-east of the La Rochelle platform (Fig. 1), protecting it from the north-eastern influence of hurricanes that were common during Late Jurassic times (Marsaglia and DeVries Klein, 1983, 1985).

5.2. Palynofacies

The high abundance of woody particles indicates proximal depositional environments (Steffen and Gorin, 1993; Tyson, 1993), which are close to the continental source. Dinocysts are principally proximate and proximo-chorate morphotypes, which are characteristic of unstable, nearshore marine paleoenvironments (Prauss, 1989). However, this assumption is empirical, and observations of modern cyst distributions do not support this interpretation (Tyson, 1995).

Four parameters describe palynofacies: the relative abundance of amorphous organic matter (AOM), which results from the degradation of marine or continental organic matter, the marine/continental component ratio (Steffen and Gorin, 1993; Tyson, 1993; Pittet and Gorin, 1997), the opaque/translucent phytoclast ratio (also called palynomacerals: PM; Summerhayes, 1987; Tyson, 1989, 1995) Pittet and Gorin, 1997, and the inertinite PM4T/PM4E ratio (Tyson, 1987). A high percentage of AOM can reflect low-energy conditions (Tyson, 1987). The marine fraction is more important in distal environments than in proximal ones. Translucent phytoclasts reflect fresher, less transported woody particles than do opaque phytoclasts. Blade-shaped PM4Ts have a better buoyancy than equidimensional PM4Es (Whitaker, 1984; Boulter and Riddick, 1986; Tyson, 1987; Van der Zwan, 1990). A higher PM4T/PM4E ratio reflects a longer transport. The marine/continental, opaque/translucent, and PM4T/PM4E ratios can be interpreted in terms of proximality–distality: a higher ratio indicates more distal depositional environments than a lower one. However, the marine/continental ratio can also be interpreted in terms of preservation. Dinocysts dominate the marine fraction. Woody particles are the essential constituents of the continental fraction. Dinocysts and other marine algae are more prone to degradation than woody particles (Bombardiere and Gorin, 1998). Therefore, a low marine/continental ratio can indicate a lower preservation state of organic matter. The opaque/translucent ratio can also indicate the state of preservation. Translucent, fresh woody particles are more prone to degradation than opaque ones (Gorin and Steffen, 1991; Hart, 1986). Organic matter-oxidation increases in high-energy, and maybe more proximal, depositional environments (Götz et al., 2005). Therefore, a high value of the opaque/translucent ratio reflects low preservation in proximal depositional environments. Only the PM4T/PM4E ratio cannot be affected by preservation. It is based on the most resistant organic particles, and only reflects particle buoyancy.

High AOM values reflect low-energy conditions, and possibly higher relative sea level. There is an exception for the two series of brown–red wackestone beds (facies 7), that show a high proportion of brown, very degraded phytoclasts. These very altered particles do not resemble to long transported and oxidised woody particles, but look like fresh woody particles reworked from the continent and rapidly buried. So, these particles can be interpreted as fresh woody particles that were reworked during a transgression. The marine/continental and the PM4T/PM4E ratios decrease from the base of the Pas section to the top of the *rupellensis* Zone (Fig. 12), despite higher values in the most distal part of the section (for instance between metres 20, 31 and 45). This decrease may result from a progressive shift from more distal to more proximal environments. A relatively similar pattern is observed in the PM4T/PM4E ratio, which shows an evolution from more distal environments in the lower part of the section to more proximal environments around the boundary between the *rupellensis* and *cymodoce* Zones, near the second erosional surface. The opaque/translucent ratio is relatively steady throughout the Pas succession, suggesting a relatively stable hydrodynamism and/or no change in organic-matter preservation. The latter is confirmed by the constant and important dinocyst degradation all along the section. There is no significant correlation between the opaque/translucent and the marine/continental ratios and between the opaque/translucent and PM4T/PM4E ratios. This suggests that the opaque/translucent ratio does not reflect proximal–distal variations. The PM4T/PM4E ratio increases during the beginning of the *cymodoce* Zone, suggesting an increase in relative sea level. The marine/continental ratio does not increase. This could be due to a preservation problem, as the marine fraction is poorly preserved all along the Pas section.

The Rocher d'Yves section shows a global decrease in the marine/continental ratio (Fig. 13) that can be interpreted as a progressive evolution towards more proximal environments. However, no significant differences were observed in the organic-matter preservation throughout the succession. Moreover, there is no correlation between the marine/continental ratio and the PM4T/PM4E ratio or the opaque/translucent ratio. On the other hand, the opaque/translucent and PM4T/PM4E ratios follow opposite trends. This relation suggests a hydrodynamic control on these ratios. When hydrodynamism increases, blade-shaped particles (PM4T) are easily transported onshore and translucent particles are easily degraded (Hart, 1986; Van der Zwan, 1990). This leads to a decrease in the PM4T/PM4E ratio and in an increase in the opaque/translucent ratio.

The comparison between the palynofacies of the two sections must be considered with caution. Values of the marine/continental ratio are lower in the Pas section than in the Rocher d'Yves section, suggesting a more proximal setting or more important degradation of organic matter. The preservation of dinocysts is clearly better in the Rocher d'Yves section, with a lower proportion of AOM than in the Pas section. This suggests that the organic-matter preservation is an important factor that explains the differences between the marine/continental ratio of the Pas and Rocher d'Yves sections. Proximal–distal variations control the PM4T/PM4E ratio in the Pas section, while they depend on hydrodynamism in the Rocher d'Yves section. The opaque/translucent ratio is affected by both preservation and hydrodynamism. Therefore, these three ratios do not allow the comparison of the two sections in terms of proximality–distality. However, the AOM content is lower in the Rocher d'Yves section than in the Pas section (Figs. 12 and 13). The high AOM content reflects low-energy conditions (Tyson, 1987). This suggests higher energy conditions in the Rocher d'Yves section than in the Pas section, and maybe shallower bathymetry or more frequent storms than in the Pas section. This is in agreement with the sedimentological interpretation, but this has to be considered with caution, as it is difficult to compare two sections separated by 2 My.

Moreover, the AOM positively correlates with the calcium carbonate content in the Pas section (Table 1). This suggests that carbonate-rich intervals reflect lower-energy conditions than marly intervals. The Rocher d'Yves section presents fewer samples than the Pas section (23 and 43, respectively), perhaps too few for a relevant comparison (Table 2).

5.3. Calcareous nannofossils

The absolute abundances of coccoliths and schizospheres are negatively correlated with the calcium carbonate content in the Pas section (Table 1). This could be due to a lower preservation of calcareous nannofossils in limestones than in marls (Thierstein and Roth, 1991; Erba, 1992; Mattioli, 1997). However, no apparent link between calcium carbonate content and nannofossil preservation is observed (Figs. 14 and 15). The Kimmeridgian deposits of the La Rochelle area are essentially mudstones. The absolute abundance of ascidian spicules in the samples is very high compared to those of coccoliths and schizospheres, and can represent most of the carbonate fraction in marly samples, which suggests that ascidians could be very important carbonate producers. However, the absolute abundance of ascidian spicules is also negatively correlated with the calcium carbonate content (Table 2). Ascidian spicules, coccoliths and schizospheres could be diluted by another source of carbonate (see Discussion). No correlations are observed for the Rocher d'Yves section (Table 1), probably for the same reason that the AOM does not correlate with calcium carbonate in the Rocher d'Yves section (see last paragraph in Section 5.2).

The absolute abundance of ascidian spicules in the second red–brown bed series is very low, and coccoliths are very scarce in 3 samples (Fig. 14, between metres 42 and 45). These samples are characterised by high calcium carbonate contents. No apparent link is observed between the calcium carbonate content and preservation. Paleoenvironmental conditions were therefore probably not suitable for calcareous nannofossils during the deposition of these beds. This point is further discussed later.

Extant ascidians are benthic organisms that live in very shallow marine environments, between 6 and 15 m depth (Moreira da Rocha and Barros de Faria, 2005). Ascidians spicules are abundant in the Pas and Rocher d'Yves sections (Figs. 14 and 15), indicating that the paleoenvironments of the two sections could approximately correspond to their living depth. However, intervals in the Rocher d'Yves section show very low absolute abundances of ascidian spicules compared to the rest of the section (Fig. 15). They could correspond to paleoenvironments that were not suitable for ascidians, above or below their living bathymetry. As paleoenvironments in the Rocher d'Yves section are more proximal than those of the Pas section, and as these low abundance intervals appear in the most proximal parts of the section (see Figs. 7 and 15), they could correspond to a paleoenvironment with a bathymetry less than 6 m depth.

W. britannica, *C. margerelii*, and *W. barnesiae/fossacincta* are considered as *r*-strategists that can live in unstable environments (Lees et al., 2005, 2006). Within this group, *W. britannica* is indicative of higher trophic conditions in surface waters than *C. margerelii* and *W. barnesiae*/

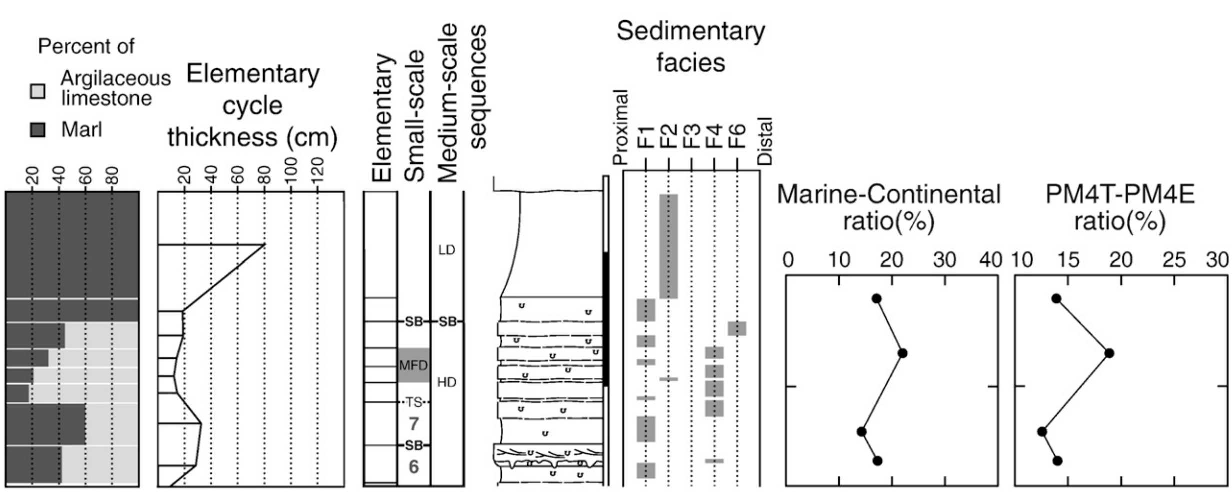

Fig. 17. An example of a small-scale sequence formed by the stacking of elementary sequences (marl–limestone alternations) from the Rocher d'Yves section.

fossacincta (Pittet and Mattioli, 2002; Olivier et al., 2004), and small-sized specimens of *W. britannica* indicate higher trophic conditions than large ones (Olivier et al., 2004; Lees et al., 2005; Giraud et al., 2006; Tremolada et al., 2006). *C. margerelii* is dominant in neritic and/or restrictive environments (Bown, 2005; Giraud et al., 2005). *W. barnesiae* is considered a eurytopic taxon (Mutterlose, 1991; Lees, 2006; Street and Bown, 2000), but still reflects lower trophic conditions than *W. britannica* and *C. margerelii* (Lees et al., 2006). Pittet and Mattioli (2002) consider *W. barnesiae* as a mesotrophic taxa. *Watznaueria biporta* seems to be adapted to low surface-water temperatures and/or low nutrient input (Hardas and Mutterlose, 2007). *Schizosphaerella* spp. reflects oligotrophic conditions (Claps et al., 1995; Cobianchi and Picotti, 2001) and/or proximal conditions in carbonate environments (Pittet and Mattioli, 2002). *Lotharingius hauffii* is indicative of meso- to eutrophic conditions (Bucefalo Palliani et al., 1998; Pittet and Mattioli, 2002), and could be abundant in proximal eutrophic paleoenvironments (Mattioli, 2006).

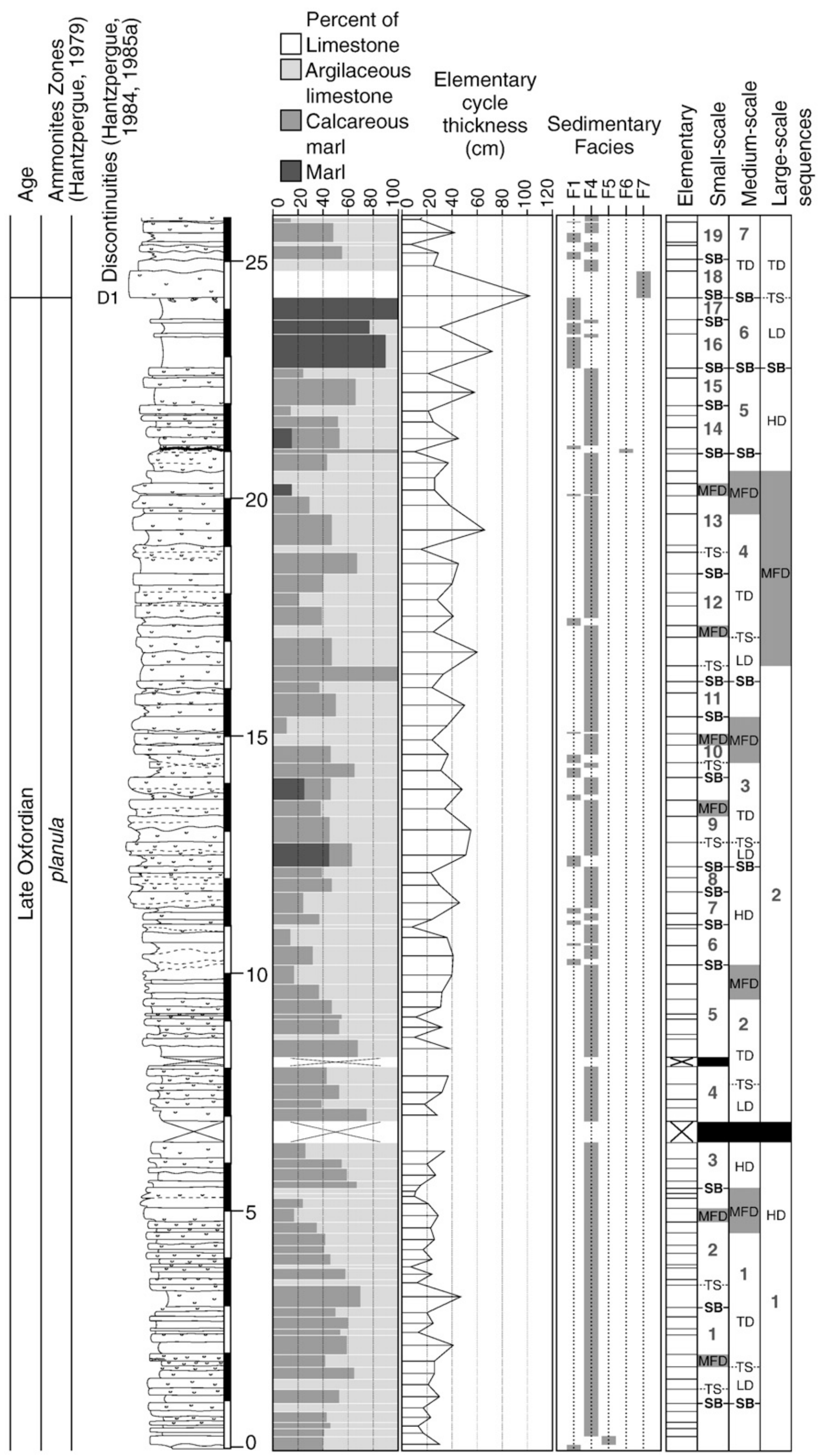

Fig. 18. Sequential interpretation of the Pas section.

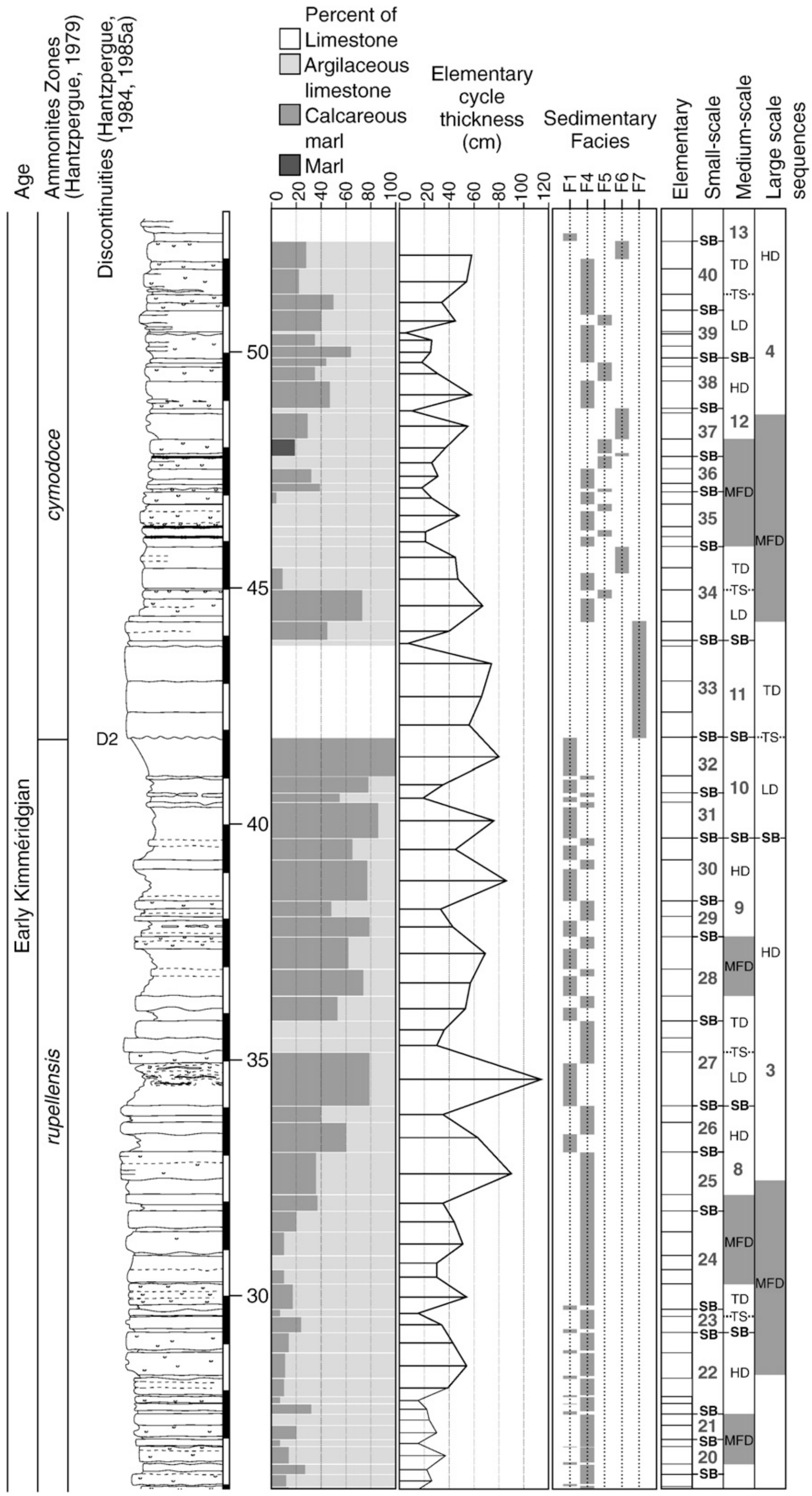

Fig. 18 (*continued*).

W. britannica is dominant in most of the samples in the lower part of the Pas section (*planula* Zone, Fig. 14), with a higher proportion of smallest-sized specimens (morphotype A). *C. margerelii* is dominant in two samples (Fig. 14, near metres 3 and 19) and presents high percentages. *W. barnesiae*/*fossacincta* and *W. biporta* are also well represented in this part of the section. Consequently, the nannofossil assemblages recognised in the lower part of the Pas section indicate unstable shallow paleoenvironments with high trophic conditions in surface waters.

The relative abundance of *L. hauffii* is higher at the end of the *planula* Zone and the beginning of the *rupellensis* Zone than in the rest of these two zones, indicating meso- to eutrophic conditions.

The relative abundance of *Schizosphaerella* spp. increases significantly from the middle to the top of the *rupellensis* Zone (Fig. 14). This increase could reflect more proximal conditions than previously.

The smallest morphotype of *W. britannica* (Morphotype A) dominates in the upper part of the Pas section, and *C. margerelii* is abundant. *L. hauffii* is frequent. The absolute abundances of both ascidian spicules and calcareous nannoplankton (coccoliths and schizospheres) are high compared to the rest of the section. This assemblage indicates higher trophic conditions in the *cymodoce* Zone than in the rest of the section.

Except for the peaks at the base of the section, which probably result from condensed intervals (no indications of higher trophic conditions, no eutrophic species, no diversification or higher abundances in micro-fossils), the absolute abundance of coccoliths and schizospheres is very close to that of the Pas section (average of 14 million coccoliths per gram of rock for the Rocher d'Yves section, and 16 million coccoliths and schizospheres for the Pas section). *C. margerelii* largely dominates the assemblages of the Rocher d'Yves section. Most samples show monospecific assemblages. The dominance of *C. margerelii* indicates neritic and/or unstable environments (Bown, 2005; Giraud et al., 2005). Furthermore, modern coccoliths show higher abundances (East China Sea, Wang and Cheng, 1985, South China Sea, Cheng, 1995), species richness, and diversity (East China Sea, Wang and Cheng, 1985, British Honduras, Scholle and Kling, 1972) in distal environments than in proximal ones. One or two species generally dominate in more proximal environments (Asian marginal seas, Okada and Honjo, 1975; Honjo, 1977). Assemblages in the Rocher d'Yves section therefore indicate more proximal paleoenvironments than those in the Pas section.

5.4. Sequence definition

A sequence-stratigraphic interpretation of the Pas and Rocher d'Yves sections is difficult because of the homogeneous sedimentary facies. Some parts of the Pas section only show two or three facies, which do not allow a definition of depositional sequences. Sedimentary facies analyses indicate that the carbonate content increases from more proximal to more distal environments (Section 5.1). The AOM relative abundance is more important in the calcareous deposits than in the marly deposits. This indicates that calcareous deposits are more distal than marly ones (Section 5.2). Moreover, decreases in marine/continental and PM4T/PM4E ratios from more calcareous to more argillaceous deposits in the Pas section also indicate that marl-dominated intervals correspond to more proximal environments than limestone-dominated intervals (Fig. 12). This trend is also visible in the calcareous nannofossil assemblages (Fig. 14). The schizosphere relative abundance increases in the *rupellensis* Zone, with a maximum in marl-dominated deposits (Section 5.3). This dominance of schizospheres suggests that marl-dominated intervals reflect more proximal conditions than limestone-dominated intervals. Calcareous nannofossil analysis reveals monospecific assemblages in the Rocher d'Yves section, indicating more proximal environments than in the Pas section, which is globally more calcareous.

On the basis of the carbonate and bioclastic contents, facies F7 should indicate the most distal environment (Section 5.1). However, in these beds, the palynofacies contain a high proportion of AOM, which results from the alteration of brown woody particles, and a low proportion of the marine fraction. Samples taken in these beds contain few calcareous nannofossils and sometimes do not include any coccoliths. These observations point to a transgressive facies. Transgression leads to fresh wood and bioclast reworking, and their accumulation results in wackestone texture. Coccoliths are produced by photosynthetic organisms, so increased turbidity due to transgression could decrease their productivity and explain their low abundances in facies F7.

Changes in the carbonate content therefore reflect variations in relative sea level. They allow several orders of depositional sequences to be defined. Elementary sequences form the smallest repetitive pattern observed in the studied sections, and correspond to marl–limestone alternations (Fig. 17). A sequence boundary corresponds to the most rapid fall of the relative sea level. As marls are more proximal than limestones, sequence boundaries correspond to the transition from a calcareous bed to a more marly bed. An argillaceous elementary sequence, formed by a thick marly bed and a thin argillaceous limestone bed, reflects more proximal conditions than a more calcareous elementary sequence, formed by a thinner marly bed and a thicker argillaceous limestone bed. Argillaceous elementary sequences are generally thicker than calcareous ones (Figs. 17 and 19).

The sequence-stratigraphic interpretation is given in Fig. 18 for the Pas section and in Fig. 19 for the Rocher d'Yves section. A small-scale sequence is formed by the stacking of elementary sequences, and contains 2 to 12 elementary sequences. Sequence boundaries (SB) of small-scale sequences correspond to the transition from a more calcareous and thinner elementary sequence, presenting distal facies, to the most argillaceous and thickest elementary sequences, corresponding to the most proximal facies (Fig. 17). A sequence boundary also corresponds to the lowest marine/continental and PM4T/PM4E ratios. Transgressive surfaces (TS) correspond to a decrease in clay content and thickness of the elementary sequences, and a shift to more distal facies. They also correspond to an increase in marine/continental and PM4T/PM4E ratios. Maximum-flooding deposits correspond to the thinnest and the most calcareous elementary sequences, the most distal sedimentary facies, and the highest marine/continental and PM4T/PM4E ratios. The SB located at the top of the small-scale sequence given in Fig. 17 is more important than the one located at the bottom (stronger sedimentary facies contrast) because it also corresponds to a medium-scale sequence boundary.

Medium- and large-scale sequences are defined according to the same rules as small-scale sequences. In the Pas section, three to five small-scale sequences form medium-scale sequences, which stack into large-scale sequences. The medium-scale sequences that surround the two erosional surfaces of the Pas section (Fig. 18) are incomplete. For instance, medium-scale sequence 10 only contains one small-scale sequence. The medium-scale sequences of the Rocher d'Yves section systematically contain 4 small-scale sequences (Fig. 19). The boundary between medium-scale sequences 1 and 2 corresponds to discontinuity D9 of Hantzpergue (1984, 1985a).

In the Pas section, large-scale sequences contain 4 medium-scale sequences (Fig. 18). Maximum-flooding deposits correspond to the thinnest and most calcareous alternations or series of alternations, while lowstand and transgressive deposits include the thickest and most argillaceous alternations. This can be explained by a more important siliciclastic input in more proximal environments than in more distal environments, resulting in thicker marl–limestone alternations. The Rocher d'Yves section does not show any complete large-scale sequence (Fig. 19).

Large-scale sequences 3 and 4 of the Pas section are characterised by stronger facies variations than large-scale sequences 1 and 2. Large-scale sequences 3 and 4 exhibit important erosive surfaces at their lowermost part (Fig. 18), which correspond to discontinuities D1 and D2 of Hantzpergue (1984, 1985a), and are interpreted as transgressive surfaces. Facies F7, which corresponds to massive brown–red wackestone beds, follows both these surfaces.

Facies F7 is a transgressive facies, and does not belong to a proximal–distal transect because it reflects particular hydrodynamical conditions (reworking of sediments by a transgression). It does not occur in the second large-scale sequence of the Pas section (Fig. 18), but appears in the third large-scale sequence (where it corresponds to a less than 1 m bed), and becomes more important in the fourth large-scale sequence (where it corresponds to five beds that reach 2 m in thickness). This increase in the proportion of facies F7 correlates with

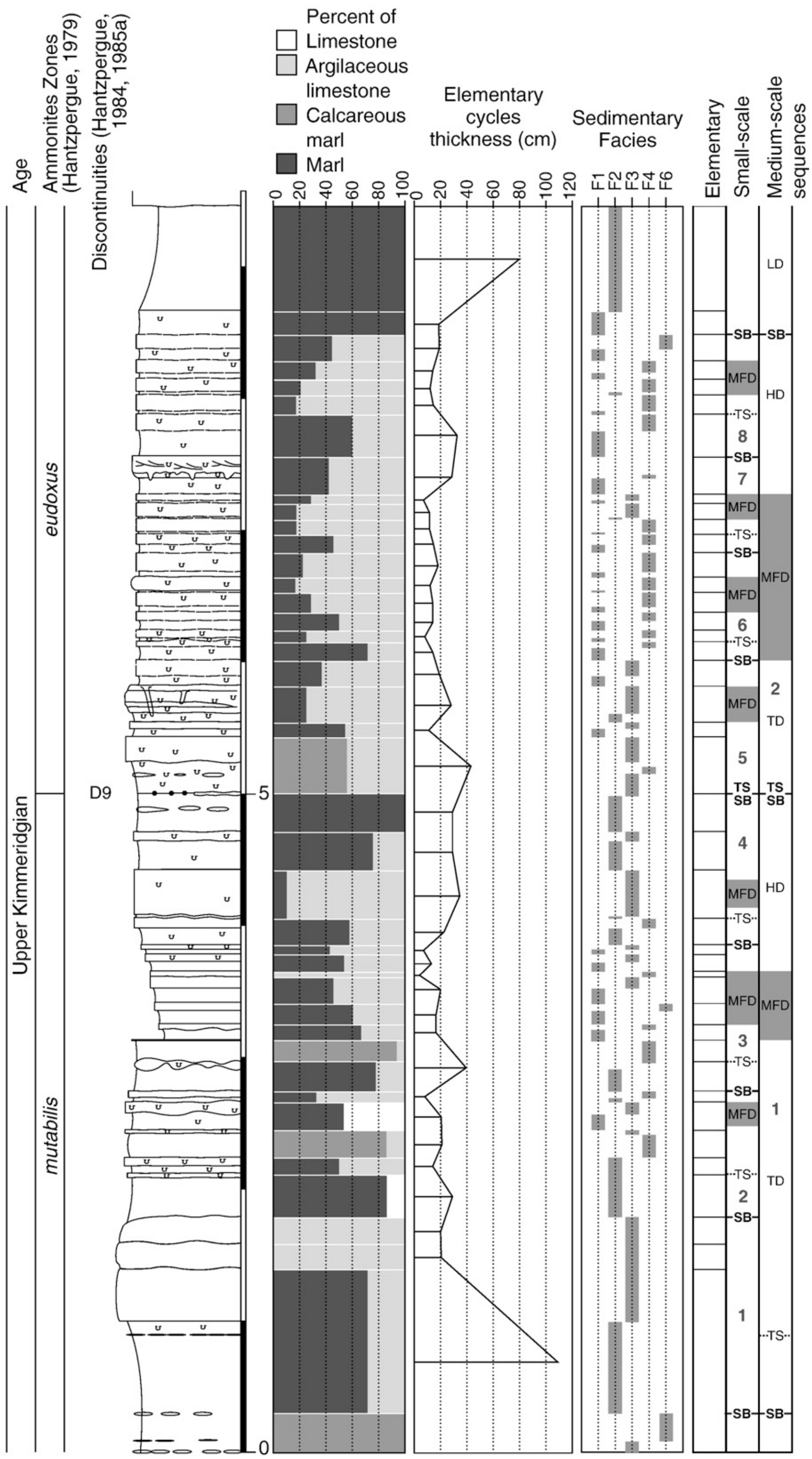

Fig. 19. Sequential interpretation of the Rocher d'Yves section.

the shift to more proximal environments between the base and the top of the Pas section, deduced from the decrease in the marine/continental and PM4T/PM4E ratios (Fig. 12), and the increase in the relative abundances of schizospheres (Fig. 14). Reworking by transgression becomes more efficient in more proximal environments, where bathymetry is lower than in more distal environments.

5.5. High-resolution correlations

Hantzpergue (1991a, 1993, 1995) interpreted D1 and D2 as third-order sequence boundaries. According to the sequence-stratigraphic chart of Ogg et al. (2008), D1 and D2 correspond to the third-order maximum-flooding surfaces of boreal sequences (Fig. 2). In the interpretation proposed in this work, D1 and D2 correspond to the transgressive surfaces of the large-scale sequences 3 and 4, respectively.

The *rupellensis* Zone of Hantzpergue (1979) almost corresponds to the sub-boreal *baylei* Zone defined by Ogg et al. (2008) (Fig. 2). In the Pas section, the *planula* Zone precedes the *rupellensis* Zone. The *planula* Zone is supposed to be a Tethyan ammonite zone (Fig. 2). In the boreal realm, the *baylei* Zone is supposed to follow the *pseudocordata* Zone, and so should be the *rupellensis* Zone of the Pas section.

According to the ammonite biostratigraphy, the large-scale sequences of the Pas section correlate with the boreal third-order sequences of Ogg et al. (2008) (Fig. 20). The base of large-scale sequence 3 is located in the *planula* Zone, and the base of large-scale sequence 4 is located in the *rupellensis* Zone (Fig. 20). Consequently, the bases of large-scale sequences 3 and 4 in the Pas section most probably correspond to the boreal third-order sequence boundaries Ox 8 and Kim 1 of Ogg et al. (2008), respectively (Fig. 20). The maximum floodings of third-order sequences Ox 8 and Kim 1 are localised in the first half of the *rupellensis* Zone and at the beginning of the *cymodoce* Zone, respectively. There is no complete large-scale sequence in the Rocher d'Yves section.

The third-order sequence boundaries of the Pas section also correlate with those defined in Oxfordian and Kimmeridgian sections (Fig. 20) from the Swiss Jura (Colombié, 2002; Colombié and Strasser, 2005; Strasser, 2007) and south-eastern France (Colombié, 2002, Colombié and Strasser, 2003, Strasser, 2007). However, the large- and

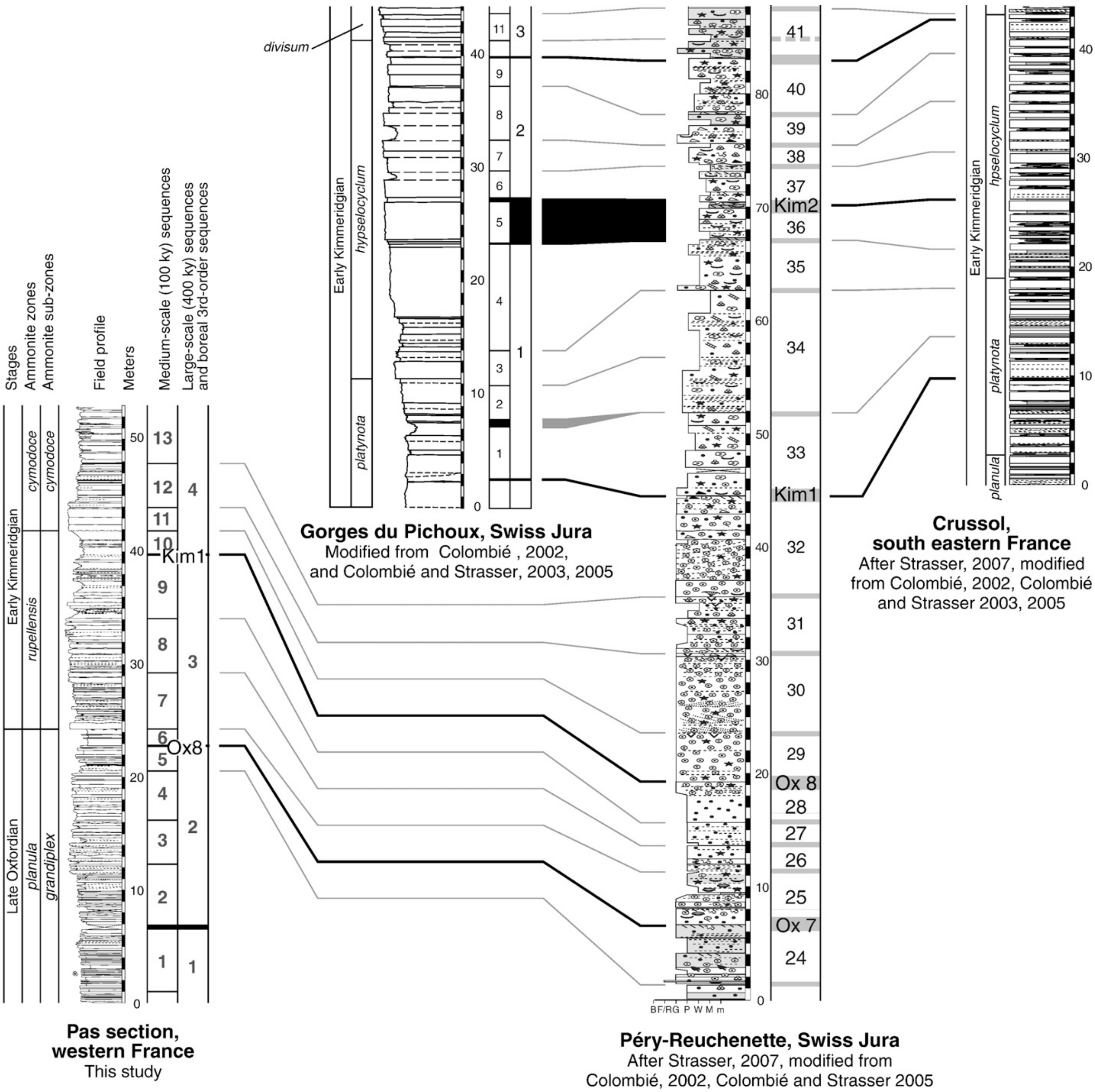

Fig. 20. Correlations of the La Rochelle sections with Tethyan sections: Crussol, Péry-Reuchenette and Gorges du Pichoux. The Crussol section extends in this study from the terminal Oxfordian to the Late Kimmeridgian (Ox 8 to Kim 4), the Péry-Reuchenette and the Gorges du Pichoux sections from the middle Oxfordian to the end of the Kimmeridgian; for practical reasons, only the parts of these sections corresponding to the La Rochelle sections are represented.

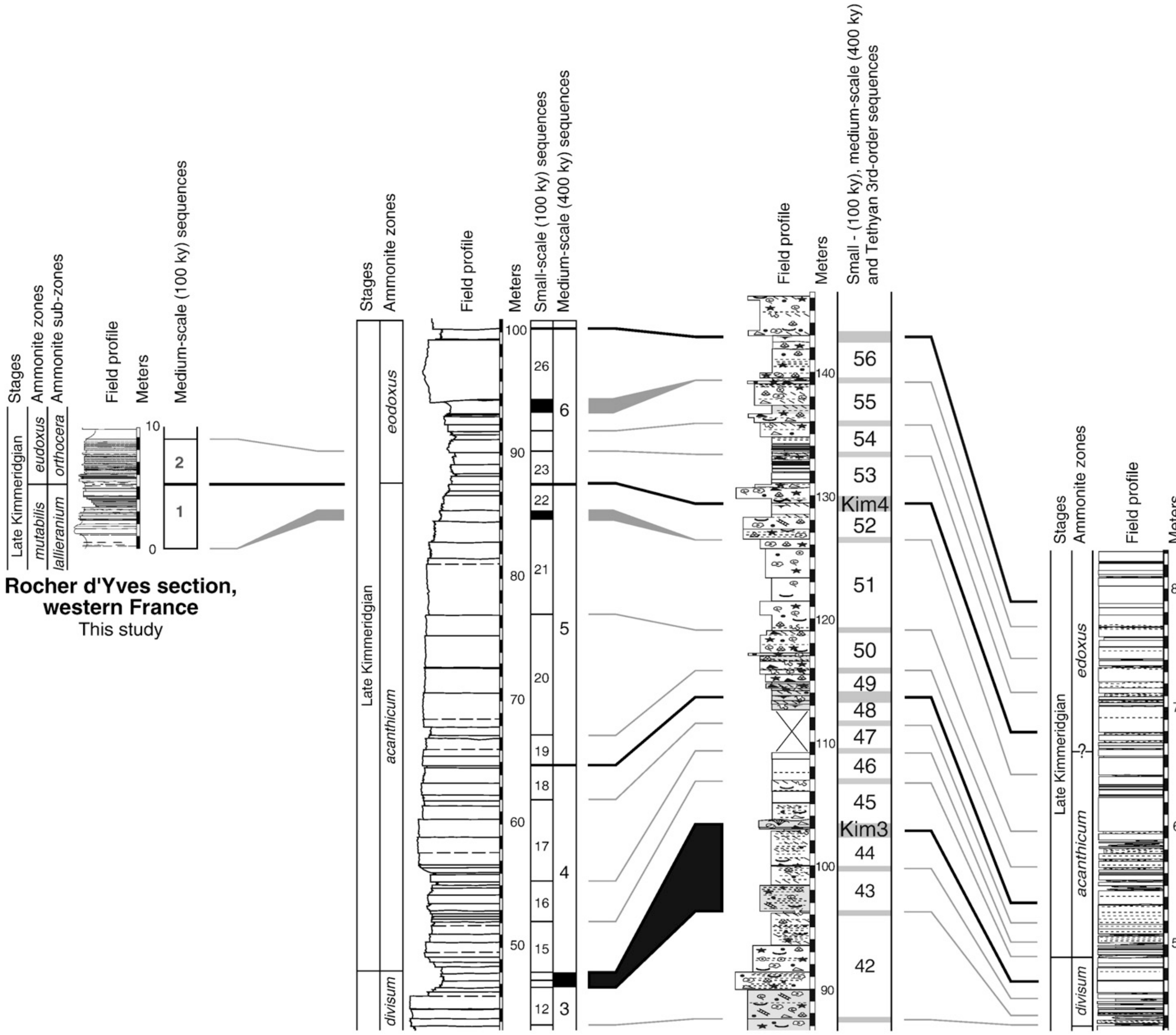

Fig. 20 (*continued*).

medium-scale sequences of the Pas and Rocher d'Yves sections correspond to medium- and small-scale sequences from the Swiss Jura and south-eastern France, respectively. Based on cyclostratigraphy, Strasser (2007) gives a duration of 400 ky for the Tethyan third-order sequences Ox 7 which is closed to the boreal third-order sequences Ox 8 defined in the Pas section, and for Ox 8, which corresponds to Kim 1 in the Pas section (Fig. 20). This suggests that sedimentation of the La Rochelle sections is orbitally controlled, and that large- and medium-scale sequences of the Pas sections correspond to 400 and 100 ky eccentricity cycle, respectively. Consequently, small-scale sequences should correspond to 20 ky precession cycle.

Ogg et al. (2008) propose a duration of 800 ky and 1.2 My for the Tethyan third-order sequences Ox 7 and Ox 8, respectively (Fig. 2). This is in contradiction with the duration based on cyclostratigraphy proposed by Strasser (2007). This suggests that the durations of the ammonite zones and third-order sequences are over-estimated in the chart of Ogg et al. (2008) for the end of the Oxfordian, or that the cyclostratigraphic interpretation is wrong.

According to ammonite biostratigraphy (Fig. 2), Tethyan third-order sequence boundary Kim 4 correlates with the base of the medium-scale sequence 2 of the Rocher d'Yves section (Fig. 20). This boundary corresponds to the major discontinuity D9 (Fig. 2) identified by Hantzpergue (1984, 1985a). As Kim 4 has a 800 ky duration in the Boreal realm, D9 probably corresponds to a 400 ky sequence boundary localised between the boreal sequence boundaries Kim 4 and Kim 5 (Fig. 2). This discontinuity includes the lowstand deposit of small-scale sequence 5.

6. Discussion

6.1. Sedimentological and paleontological aspects

The ascidian spicules represent an important carbonate fraction, but are diluted, with coccoliths and schizospheres, by another source of carbonate mud. Coral reefs are present in the La Rochelle platform during the Late Jurassic, located along the Hercynian faults (Hantzpergue, 1985b, 1988). Carbonate production increases during highstand periods, leading to more calcareous deposits (Neumann and McIntyre, 1985).

Colombié et al. (2007) worked in the Late Kimmeridgian–Early Tithonian of the Aquitaine Basin. They propose that this mud is produced by corals and other carbonate-producing organisms during highstand periods, and redistributed by storms all over the platform. Coral reef emersion during lowstand periods leads to a decrease in carbonate production. This could also explain why the maximum-flooding and highstand deposits are dominated by carbonate mud, and that the lowstand deposits are dominated by clay.

6.2. Evolution of the La Rochelle sedimentary system

According to Ogg et al. (2008), the Late Kimmeridgian corresponds to a second-order maximum flooding (Fig. 2). Hantzpergue (1993, 1995) defined third-order sequences in the La Rochelle sections. He assumed that the "virgulian" facies, which is characteristic of the Rocher d'Yves section, indicates the second-order maximum flooding. Jacquin et al. (1998) gave the same interpretation of this facies in the Channel Basin. However, the facies encountered in the Rocher d'Yves section generally indicate more proximal depositional environments than in the Pas section. In this study, the *N. virgula* facies (F2 and F3) correspond to more proximal environments than those of the Channel Basin. However, the Rocher d'Yves section is located close to the second-order maximum flooding, and should be more distal than the Pas section, which formed during the beginning of the second-order transgression. This implies that the sediment supply was higher than the accommodation space creation during the second-order sea-level rise, leading to the progradation of the La Rochelle platform from the Early to the Late Kimmeridgian.

Such a phenomenon was also observed by Colombié and Strasser (2003), with a progradation of the Jura platform during the Late Kimmeridgian, but there was the result of a higher carbonate production. The Rocher d'Yves section is globally more argillaceous than the Pas section. An increase in carbonate production cannot explain the progradation of the La Rochelle platform. An increase in siliciclastic input from the continent is not a good explanation either, as the Late Kimmeridgian was more arid than the Early Kimmeridgian (Abbink et al., 2001).

Consequently, this progradation could have a tectonic origin. If subsidence slows down, the platform can prograde. This was observed in the Kimmeridgian of the Lusitanian Basin: a tectonically induced marine sea-level drop led to a rapid and complete filling of marine parts of the Lusitanian Basin, mainly by clastic sediments (Leinfelder, 1987). This was also observed in the Iberian Basin by Bádenas and Aurell (2001a), where basin uplift, due to the onset of the Late Jurassic–Early Cretaceous rifting stage of the Atlantic Ocean, led to a basinward progradation of the shorelines. The Jurassic in the Aquitaine Basin, and more largely in the Bay of Biscay, was a relatively calm tectonic period (Montadert and Winnock, 1971). However, the active tectonic phase that preceded the opening of the North Atlantic and corresponded to the rotation of the Iberian block during the lower Cretaceous (García-Mondéjar, 1996), started during the Late Jurassic (Laughton, 1972; De Graciansky and Wylie Poag, 1985). This led in the Aquitaine Basin to an abrupt increase in subsidence during the Early Kimmeridgian, rapidly compensated by thermally-induced basement uplift until the Late Kimmeridgian and the Tithonian.

7. Conclusions

The Pas and Rocher d'Yves sections correspond to shallow open-marine environments. The combination of sedimentological, palynofacies and calcareous nannofossil analyses allow a partitioning of sedimentary facies along a proximal–distal transect. Distal depositional environments are more calcareous and contain more abundant and more diversified bioclasts than proximal ones. Siliciclastic input from the continent resulted in proximal argillaceous deposits thicker than distal carbonate deposits.

Sediments are essentially mudstones, but the two sections contain abundant bioclastic and/or peloidal deposits. These deposits display wackestone to wacke-pack-grainstone textures, cross- or planar-stratification, and are grain-sorted. Their presence in shallow-water deposits and their sharp bases indicate that they are storm deposits. The Pas and Rocher d'Yves sections therefore correspond to low-energy environments with frequent storm events.

A high-resolution sequence-stratigraphic interpretation is proposed for the two sections. Correlations with other boreal and Tethyan sections provide further support for this interpretation. The sequence-stratigraphic interpretation was used to establish a precise cyclostratigraphic framework, revealing that sedimentation was controlled by precession and the two eccentricity cycles. Large- and medium-scale sequences in the La Rochelle sections correspond to 400 and 100 ky eccentricity cycles, respectively. Consequently, the duration of small-scale sequences should correspond to the precession cycle (20 ky), and elementary sequences should be shorter than 20 ky. The cyclostratigraphic interpretation proposed in this study is the same as the one established in the Iberian ranges (eastern Spain) by Bádenas et al. (2003), who proposed a duration of 20 ky for bundles (equivalent to small-scale sequences) and 100 ky for sets of bundles (equivalent to medium-scale sequences).

This study reveals a progradation of the La Rochelle platform during the Kimmeridgian, despite the fact that the Kimmeridgian was a period of global sea-level rise. A rapid increase in subsidence during the beginning of the Kimmeridgian is followed by a basement uplift in the Aquitaine Basin during the rest of the stage, leading to a loss in accommodation space and the progradation of the platform. These tectonic movements correspond to the first steps of the Atlantic Ocean opening. Consequently, if orbital cycles control high-frequency sequences (tens and hundreds of thousands of years), tectonics seems to be the essential factor controlling the formation of low-frequency sequences (millions of years).

Acknowledgments

We are grateful to Dr Beatriz Bádenas and Pr André Strasser, whose comments considerably improved the manuscript. This research was financed by the UMR 5125 PEPS, the CNRS program "ECLIPSE II," and the MAIF Foundation. Damien Carcel thanks the IFR 41 for their funding for his PhD study. Damien Carcel and Claude Colombié also thank the CNFG for their travel grant, allowing them to participate in the 25th IAS meeting of sedimentology (Patras, Greece). Finally, the authors are indebted to Dr. Jean-Jaques Cornée (Montpellier University, France) for his useful comments during the writing of this manuscript.

Appendix A. Observed coccolith species

Ascidian spicules

Didemnum spp.

Coccoliths

Biscutum dorsetensis (Varol and Girgis, 1994) Bown and Cooper *in* Bown, 1998
Crepidolithus perforata (Medd, 1979) Grün and Zweili, 1980
Cyclagelosphaera margerelii Noël, 1965
Cyclagelosphaera tubulata (Grün and Zweili, 1980) Cooper, 1987
Cyclagelosphaera wiedmanni Reale and Monechi, 1994
Diazomatolithus lehmanii Noël, 1965
Discorhabdus criotus Bown, 1987
Ethmorhabdus gallicus Noël, 1965
Lotharingius contractus Bown and Cooper, 1989
Lotharingius crucicentralis (Medd, 1971) Grün and Zweili, 1980

Lotharingius hauffii Grün and Zweili *in* Grün et al., 1974
Lotharingius sigillatus (Stradner, 1961) Prins *in* Grün et al., 1974
Miravetesina favula Grün *in* Grün and Allemann, 1975
Nannoconus compressus Bralower and Thierstein *in* Bralower et al., 1989
Parhabdolithus liasicus Deflandre *in* Grassé, 1952
Podorhabdus grassei Noël, 1965
Triscutum expansus (Medd, 1979) Dockerill, 1987
Triscutum sullivanii de Kaenel and Bergen, 1993
Tubirhabdus patulus Rood et al., 1973
Watznaueria barnesiae (Black, 1959) Perch-Nielsen, 1968
Watznaueria biporta Buckry, 1969
Watznaueria britannica (Stradner, 1963) Reinhardt, 1964
Watznaueria communis Reinhardt, 1964
Watznaueria fossacincta (Black, 1971) Bown *in* Bown and Cooper, 1989
Watznaueria manivitiae Buckry, 1973
Watznaueria manivitiae/britannica Giraud et al., *2009*
Watznaueria ovata Buckry, 1979
Zeugrhabdotus embergeri (Noél, 1958) Perch-Nielsen, 1984
Zeugrhabdotus erectus (Deflandre *in* Deflandre and Fert, 1954) Reinhardt, 1965
Incertae sedis: *Schizosphaerella* spp.

References

Abbink, O., Targarona, J., Brinkhuis, H., Visscher, H., 2001. Late Jurassic to earliest Cretaceous palaeoclimatic evolution of the southern North Sea. Global and Planetary Change 30 (3-4), 231–256.

Aigner, T., 1982. Calcareous Tempestites: Storm-dominated Stratification in Upper Muschelkalk Limestones (Middle Trias, SW-Germany). In: Einsele, G., Seilacher, A. (Eds.), Cyclic and Event Stratification. Springer-Verlag, Berlin, Federal Republic of Germany, pp. 180–198.

Atrops, F., Gygi, R., Matyja, B., Wierzbowski, A., 1993. The Amoeboceras faunas in the Middle Oxfordian–lowermost Kimmeridgian, submediterranean succession, and their correlation value. Acta Geologica Polonica 43 (3–4), 229–249.

Bádenas, B., Aurell, M., 2001a. Kimmeridgian palaeogeography and basin evolution of northeastern Iberia. Palaeogeography, Palaeoclimatology, Palaeoecology 168 (3–4), 291–310.

Bádenas, B., Aurell, M., 2001b. Proximal–distal facies relationships and sedimentary processes in a storm dominated carbonate ramp (Kimmeridgian, northwest of the Iberian Ranges, Spain). Sedimentary Geology 139 (3–4), 319–340.

Bádenas, B., Aurell, M., Rodriguez-Tovar, F.J., Pardo-Iguzquiza, E., 2003. Sequence stratigraphy and bedding rhythms of an outer ramp limestone succession (Late Kimmeridgian, Northeast Spain). Sedimentary Geology 161 (1–2), 153–174.

Bombardiere, L., Gorin, G.E., 1998. Sedimentary organic matter in condensed sections from distal oxic environments: examples from the Mesozoic of SE France. Sedimentology 45 (4), 771–788.

Bornemann, A., Mutterlose, J., 2006. Size analyses of the coccolith species Biscutum constans and *Watznaueria barnesiae* from the Late Albian "Niveau Breistroffer" (SE France): taxonomic and palaeoecological implications. Geobios 39 (5), 599–615.

Boulter, M.C., Riddick, A., 1986. Classification and analysis of palynodebris from the Palaeocene sediments of the Forties Field. Sedimentology 33 (6), 871–886.

Bown, P.R., 2005. Selective calcareous nannoplankton survivorship at the Cretaceous–Tertiary boundary. Geology 33 (8), 653–656.

Bucefalo Palliani, R., Cirilli, S., Mattioli, E., 1998. Phytoplankton response and geochemical evidence of the lower Toarcian relative sea level rise in the Umbria–Marche basin (Central Italy). Palaeogeography, Palaeoclimatology, Palaeoecology 142 (1–2), 33–50.

Burchette, T.P., Wright, V.P., 1992. Carbonate ramp depositional systems. Sedimentary Geology 79 (1–4), 3–57.

Cariou, E., 1972. L'Oxfordien au Nord de Poitiers. La limite Oxfordien–Kimméridgien en Poitou-Charentes. Comptes Rendus de l'Académie des Sciences de Paris 275, 2607–2609.

Cariou, E., Hantzpergue, P., 1997. Groupe Français d'étude du Jurassique: Biostratigraphie du jurassique ouest-européen et méditerranéen — Zonations parallèles et distribution des invertébrés et microfossiles. Bulletin du centre de recherches Elf Exploration Production, Pau, France 17.

Cheng, X., 1995. Distribution of dominant species and abundance of nannofossils in surface sediments of the central and northern parts of the South China Sea — comparison and discussion. Acta Oceanologica Sinica 14 (4), 525–535.

Claps, M., Erba, E., Masetti, D., Melchiorri, F., 1995. Milankovitch-type cycles recorded in Toarcian black shales from the Belluno Trough (Southern Alps, Italy). Memorie Scienze Geologiche, Padova 47, 179–188.

Cobianchi, M., Picotti, V., 2001. Sedimentary and biological response to sea-level and palaeoceanographic changes of a Lower-Middle Jurassic Tethyan platform margin (Southern Alps, Italy). Palaeogeography, Palaeoclimatology, Palaeoecology 169 (3–4), 219–244.

Colombié, C., 2002. Sédimentologie, stratigraphie séquentielle et cyclostratigraphie du Kimméridgien du Jura suisse et du Bassin vocontien (France): relations plate-forme — bassin et facteurs déterminants. Ph.D. thesis, Université de Fribourg, Suisse.

Colombié, C., Rameil, N., 2007. Tethyan-to-boreal correlation in the Kimmeridgian using high-resolution sequence stratigraphy (Vocontian Basin, Swiss Jura, Boulonnais, Dorset). International Journal of Earth Sciences 96 (3), 567–591.

Colombié, C., Schnyder, J., Carcel, D., 2007. Marl–Limestone Couplets in the Late Jurassic of Western France: Cycles or Event Beds? Book of Abstracts. 25th IAS Meeting of Sedimentology, p. 67.

Colombié, C., Strasser, A., 2003. Depositional sequences in the Kimmeridgian of the Vocontian Basin (France) controlled by carbonate export from shallow-water platforms. Geobios 36 (6), 675–683.

Colombié, C., Strasser, A., 2005. Facies, cycles, and controls on the evolution of a keep-up carbonate platform (Kimmeridgian, Swiss Jura). Sedimentology 52 (6), 1207–1227.

Courtinat, B., Piriou, S., Rio, M., 2003. Phytoclasts in palynofacies definition: the example of Rhaetian sedimentary organic matter in SE France. Revue de Micropaleontologie 46 (1), 11–21.

De Graciansky, P.-C., Wylie Poag, C., 1985. Geological History of Goban Spur, Northwest Europe Continental Margin. Initial Reports of the Deep Sea Drilling Project, vol. 80. Texas A & M University, Ocean Drilling Program, College Station, TX, United States, pp. 1187–1216. Ch. 58.

Delfaud, J., Servant, M., 1971. Essai d'interprétation des récifs du Portlandien Nord-Aquitain. Bulletin de la Société Linnéenne de Bordeaux 1 (1), 7–23.

Einsele, G., Chough, S.K., Shiki, T., 1996. Depositional events and their records — an introduction. Sedimentary Geology 104 (1–4), 1–9.

Einsele, G., Ricken, W., Seilacher, A., 1991. Cycles and Events in Stratigraphy — Basic Concepts and Terms. In: Einsele, G., Ricken, W., Seilacher, A. (Eds.), Cycles and Events in Stratigraphy. Springer-Verlag, Berlin, pp. 23–47. Ch. 1.

Erba, E., 1992. Calcareous nannofossil distribution in pelagic rhythmic sediments (Aptian–Albian Piobbico Core, Central Italy). Rivista Italiana di Paleontologia e Stratigrafia 97 (3–4), 455–484.

Flügel, E., 2004. Microfacies of Carbonate Rocks: Analysis, Interpretation and Application. Springer, Berlin.

Fürsich, F.T., Oschmann, W., 1986. Storm shell beds of *Nanogyra virgula* in the upper Jurassic of France. Neues Jahrbuch für Geologie und Palaontologie 172 (2), 141–161.

Gagan, M.K., Chivas, A.R., Herczeg, A.L., 1990. Shelf-wide erosion, deposition, and suspended sediment transport during Cyclone Winifred, central Great Barrier Reef, Australia. Journal of Sedimentary Research 60 (3), 456–470.

Gagan, M.K., Johnson, D.P., Carter, R.M., 1988. The Cyclone Winifred storm bed, central Great Barrier Reef shelf, Australia. Journal of Sedimentary Research 58 (5), 845–856.

García-Mondéjar, J., 1996. Plate reconstruction of the Bay of Biscay. Geology 24 (7), 635–638.

Geisen, M., Bollmann, J., Herrle, J.O., Mutterlose, J., Young, J.R., 1999. Calibration of the random settling technique for calculation of absolute abundances of calcareous nannoplankton. Micropaleontology 45 (4), 437–442.

Giraud, F., Courtinat, B., Garcia, J.-P., Baudin, F., Guillocheau, F., Dromart, G., Atrops, F., Collete, C., 2005. Palynofacies and calcareous nannofossils in the Upper Kimmeridgian, southeastern Paris basin (France). Bulletin. Société Géologique de France 176 (5), 457–466.

Giraud, F., Pittet, B., Mattioli, E., Audouin, V., 2006. Paleoenvironmental controls on the morphology and abundance of the coccolith *Watznaueria britannica* (Late Jurassic, southern Germany). Marine Micropaleontology 60 (3), 205–225.

Gorin, G.E., Steffen, D., 1991. Organic facies as a tool for recording eustatic variations in marine fine-grained carbonate — example of the Berriasian stratotype at Berris (Ardèche, SE France). Palaeogeography, Palaeoclimatology, Palaeoecology 85 (3–4), 303–320.

Götz, A.E., Szulc, J., Feist-Burkhardt, S., 2005. Distribution of sedimentary organic matter in Anisian carbonate series of S Poland: evidence of third-order sea-level fluctuations. International Journal of Earth Sciences 94 (2), 267–274.

Gradstein, F.M., Agterberg, F.P., Ogg, J.G., Hardenbol, J., 1994. A Mesozoic time scale. Journal of Geophysical Research 99 (B12), 24051–24074.

Hantzpergue, P., 1979. Biostratigraphie du Jurassique supérieur Nord-Aquitain. Bulletin. Société Géologique de France 21 (6), 715–725.

Hantzpergue, P., 1984. Greater Sedimentary Unconformities in the Western European Kimmeridgian: Relations between Sedimentary and Biologic Events. International Symposium on Jurassic Stratigraphy III. Copenhagen, pp. 685–694.

Hantzpergue, P., 1985a. Les discontinuités sédimentaires majeures dans le Kimméridgien français: Chronologie, extension et corrélations dans les bassins Ouest-Européens. Geobios 18 (2), 179–194.

Hantzpergue, P., 1985b. L'héritage hercynien dans la paléogéographie récifale du Jurassique supérieur nord-aquitain (France). Comptes rendus de l'Académie des sciences 301 (15), 1147–1150.

Hantzpergue, P., 1988. Les plate-formes récifales du Jurassique Nord-Aquitain. Laboratoire de Géologie Stratigraphique et Structurale, Université de Poitiers, France.

Hantzpergue, P., 1989. Les ammonites kimméridgiennes du haut-fond d'Europe Occidentale. Biochronologie, Systématique, Évolution Paléobiogéographie. Cahiers paléontologiques du CNRS, 428.

Hantzpergue, P., 1991a. Biogéographie des ammonites et variations du niveau marin: apport de la stratigraphie séquentielle dans l'analyse des peuplements du Kimméridgien nord-Aquitain. Geobios 24 (1), 59–64.

Hantzpergue, P., 1991b. Différenciation paléobiogéographique d'une faune d'ammonites dans l'horizon à Ardescia pseudolictor (zone à Cymodoce) du Kimméridgien nord-Aquitain. Geobios 24 (4), 423–433.
Hantzpergue, P., 1993. Biogéographie des ammonites et variations du niveau marin: analyse quantitative des peuplements du Kimméridgien ouest-européen. Comptes rendus de l'Académie des sciences 317 (4), 493–498.
Hantzpergue, P., 1995. Faunal trends and sea-level changes: biogeographic patterns of Kimmeridgian ammonites on the Western European Shelf. Geologische Rundschau 84 (2), 245–254.
Hantzpergue, P., Maire, P., 1981. Les plates-formes de l'Aunis et de l'Angoumois au Jurassique supérieur: caractères sédimentologiques et paléogéographie. Bulletin. Société Géologique de France 23 (5), 493–500.
Hardas, P., Mutterlose, J., 2007. Calcareous nannofossil assemblages of Oceanic Anoxic Event 2 in the equatorial Atlantic: evidence of an eutrophication event. Marine Micropaleontology 66 (1), 52–69.
Hart, G.F., 1986. Origin and classification of organic matter in clastic systems. Palynology 10, 1–23.
Honjo, S., 1977. Biogeography and Provincialism of Living Coccolithophorids in the Pacific Ocean. In: Ramsay, A.T.S. (Ed.), Oceanic Micropaleontology, Vol. 2. Academic Press, London, pp. 951–972.
Jacquin, T., Dardeau, G., Durlet, C., De Graciansky, P.-C., Hantzpergue, P., 1998. The North Sea Cycle: An Overview of Lower Jurassic 2nd Order Transgressive/Regressive Facies Cycles in Western Europe. In: De Graciansky, P.-C., Hardenbol, J., Jacquin, T., Vail, P.R. (Eds.), Mesozoic and Cenozoic Sequence Stratigraphy of European Basins: SEPM special publications, vol.60, pp. 445–479.
Lafuste, J., 1955. Sur l'importance relative des organismes constructeurs des récifs séquaniens d'Angoulins-sur-Mer. Compte Rendu. Sommaire des Séances. Société Géologique de France 7, 130–131.
Laughton, A.S., 1972. The Southern Labrador Sea — A Key to the Mesozoic and Early Tertiary Evolution of the North Atlantic. Initial Reports of the Deep Sea Drilling Project, vol. 12. Texas A & M University, Ocean Drilling Program, College Station, TX, United States, pp. 1155–1179. Ch. 20.
Lécuyer, C., Picard, S., Garcia, J.-P., Sheppard, S.M.F., Grandjean, P., Dromart, G., 2003. Thermal evolution of Tethyan surface waters during the Middle–Late Jurassic: evidence from $\delta^{18}O$ values of marine fish teeth. Paleoceanography 18 (3), 1076–1092.
Lees, J.A., Bown, P.R., Mattioli, E., 2005. Problems with proxies? Cautionary tales of calcareous nannofossil paleoenvironmental indicators. Micropaleontology 51 (4), 333–343.
Lees, J.A., Bown, P.R., Young, J.R., 2006. Photic zone palaeoenvironments of the Kimmeridge Clay Formation (Upper Jurassic, UK) suggested by calcareous nannoplankton palaeoecology; causes and consequence of marine organic carbon burial through time. Palaeogeography, Palaeoclimatology, Palaeoecology 235 (1–3), 110–134.
Lees, J.A., Bown, P.R., Young, J.R., Riding, J.B., 2004. Evidence for annual records of phytoplankton productivity in the Kimmeridge Clay Formation coccolith stone bands (Upper Jurassic, Dorset, UK); calcareous nannofossil palaeoecology and palaeocenographic reconstructions. Marine Micropaleontology 52 (1–4), 29–49.
Leinfelder, R.R., 1987. Multifactorial control of sedimentation patterns in an ocean marginal basin: the Lusitanian Basin (Portugal) during the Kimmeridgian and Tithonian. International Journal of Earth Sciences 76 (2), 599–631.
Marsaglia, K.M., DeVries Klein, G., 1983. The paleogeography of paleozoic and mesozoic storm depositional systems. Journal of Geology 91 (2), 117–142.
Marsaglia, K.M., DeVries Klein, G., 1985. The paleogeography of Paleozoic and Mesozoic storm depositional systems: a reply. Journal of Geology 93 (1), 91–94.
Mattioli, E., 1997. Nannoplankton productivity and diagenesis in the rhythmically bedded Toarcian–Aalenian Fiuminata section (Umbria–Marche Apennine, central Italy). Palaeogeography, Palaeoclimatology, Palaeoecology 130 (1–4), 113–133.
Mattioli, E., 2006. Le nannoplancton calcaire durant l'événement anoxique du Toarcien inférieur: implications pour la paléocéanographie de la Téthys occidentale. Habilitation à Diriger des Recherches, Université Claude Bernard Lyon 1, France.
Montadert, L., Winnock, E., 1971. L'histoire structurale du Golfe de Gascogne. Histoire Structurale du Golfe de Gascogne, Tome 2, 16. Institut Français du Pétrole, pp. 1–18. Ch. VI.
Moreira da Rocha, R., Barros de Faria, S., 2005. Ascidians at Currais Islands, Paraná, Brazil: taxonomy and distribution. Biota Neotropica 5 (2), 1–19.
Mutterlose, J., 1991. Das Verteilungs und Migrationsmuter des kalkigen Nannoplanktons in der borealen Unterkreide (Valangin-Apt). Paläeontographica B 221, 27–152.
Neumann, A.C., McIntyre, I.G., 1985. Reef Response to Sea-level Rise: Keep-up, Catch-up or Give-up. Proceedings of the 5th International Coral Reef Congress, vol. 3, pp. 105–110. Tahiti.
Normand, M., 1970. Stratigraphie de la série du Jurassique supérieur du littoral charentais au Nord de La Rochelle. Annales de la Société des Sciences Naturelles de Charente-Maritime 5 (2), 50–69.
Normand, M., 1971. Tectonique de la série du Jurassique supérieur du littoral charentais au Nord de La Rochelle. Annales de la Société des Sciences Naturelles de Charente-Maritime 5 (3), 140–149.
Ogg, G., Ogg, J.G., Gradstein, F.M., 2008. The Concise Geologic Time Scale. Cambridge University Press, Cambridge, United Kingdom.
Okada, H., Honjo, S., 1975. Distribution of coccolithophores in marginal seas along the western Pacific Ocean and in the Red Sea. Marine Biology 31 (3), 271–285.
Olivier, N., Hantzpergue, P., Gaillard, C., Pittet, B., Leinfelder, R.R., Schmid, D.U., Werner, W., 2003. Microbialite morphology, structure and growth: a model of the Upper Jurassic reefs of the Chay Peninsula (Western France). Palaeogeography, Palaeoclimatology, Palaeoecology 193 (3–4), 383–404.
Olivier, N., Pittet, B., Mattioli, E., 2004. Palaeoenvironmental control on sponge-microbialite reefs and contemporaneous deep-shelf marl–limestone deposition (Late Oxfordian, southern Germany). Palaeogeography, Palaeoclimatology, Palaeoecology 212 (3–4), 233–263.
Olivier, N., Pittet, B., Werner, W., Hantzpergue, P., Gaillard, C., 2008. Facies distribution and coral-microbialite reef development on a low-energy carbonate ramp (Chay Peninsula, Kimmeridgian, western France). Sedimentary Geology 205 (1–2), 14–33.
Pittet, B., Gorin, G.E., 1997. Distribution of sedimentary organic matter in a mixed carbonate siliciclastic platform environment: Oxfordian of the Swiss Jura Mountains. Sedimentology 44 (5), 915–937.
Pittet, B., Mattioli, E., 2002. The carbonate signal and calcareous nannofossil distribution in an Upper Jurassic section (Balingen–Tieringen, Late Oxfordian, southern Germany). Palaeogeography, Palaeoclimatology, Palaeoecology 179 (1–2), 71–96.
Prauss, M., 1989. Dynozysten stratigraphie und palynofazies im Oberem Lias und Dogger von NW Deutschland. Paläontographica Abteilung B: Paläophytologie 214, 1–4.
Reading, H.G., Burchette, T.P., 1996. Shallow Water Carbonate Environments, In: Reading, H.G. (Ed.), Sedimentary Environments: Processes, Facies and Stratigraphy, 3rd ed. Blackwell Science, Oxford, pp. 325–394.
Scholle, P.A., Kling, S.A., 1972. Southern British Honduras; lagoonal coccolith ooze. Journal of Sedimentary Petrology 42 (1), 195–204.
Steffen, D., Gorin, G.E., 1993. Palynofacies of the Upper Tithonian — Berriasian deep-sea carbonates in the Vocontian Trough (SE France). Bulletin. Centres de Recherches Exploration-Production Elf-Aquitaine 17, 235–247.
Strasser, A., 2007. Astronomical time scale for the Middle Oxfordian to Late Kimmeridgian in the Swiss and French Jura Mountains. Swiss Journal of Geosciences 100 (3), 1661–8726.
Strasser, A., Pittet, B., Hillgärtner, H., Pasquier, J.-B., 1999. Depositional sequences in shallow carbonate-dominated sedimentary systems: concepts for a high-resolution analysis. Sedimentary Geology 128 (3–4), 201–221.
Street, C., Bown, P.R., 2000. Palaeobiogeography of Early Cretaceous (Berriasian–Barremian) calcareous nannoplankton. Marine Micropaleontology 39 (1–4), 265–291.
Summerhayes, C.P., 1987. Organic-rich Cretaceous Sediments from the North Atlantic. In: Brooks, J., Fleet, A.J. (Eds.), Marine Petroleum Source Rocks, Vol. 26. Geological Society Special Publication, London, pp. 301–316.
Thierry, J., 2000. Early Kimmeridgian. In: Dercourt, J., Gaetani, M., Vrielynck, B., Barrier, E., Biju-Duval, B., Brunet, M.F., Cadet, J.P., Crasquin, S., Sandulescu, M. (Eds.), Atlas Peri-Tethys of Palaeoenvironmental Maps. Commission for the Geological Map of the World, Paris, France.
Thierstein, H.R., Roth, P.H., 1991. Stable isotopic and carbonate cyclicity in Lower Cretaceous deep-sea sediments: dominance of diagenetic effects. Marine Geology 97 (1–2), 1–34.
Tremolada, F., Bornemann, A., Bralower, T.J., Koeberl, C., Van de Schootbrugge, B., 2006. Paleoceanographic changes across the Jurassic/Cretaceous boundary: the calcareous phytoplankton response. Earth and Planetary Science Letters 241 (3–4), 361–371.
Tucker, M.E., Wright, V.P., 1990. Carbonate Sedimentology. Blackwell Scientific Publications, Oxford.
Tyson, R.V., 1987. The Genesis and Palynofacies Characteristics of Marine Petroleum Source Rocks. In: Brooks, J., Fleet, A.J. (Eds.), Marine Petroleum Source Rocks, vol.26. Geological Society Special Publication, London, pp. 47–67.
Tyson, R.V., 1989. Late Jurassic Palynofacies Trends, Piper and Kimmeridge Clay Formations, UK Onshore and Northern North Sea. In: Batten, D.J., Keen, M.C. (Eds.), Northwest European Micropalaeontology and Palynology. British Micropal Soc. Series, Ellis Horwood, Chichester, pp. 135–172.
Tyson, R.V., 1993. Palynofacies Analysis. In: Jenkins, D.G. (Ed.), Applied Micropalaeontology. Kluwer, Dordretch, pp. 153–191.
Tyson, R.V., 1995. Sedimentary Organic Matter: Organic Facies and Palynofacies. Chapman & Hall, London.
Vail, P.R., 1987. Seismic Stratigraphy Interpretation Procedure. In: Bally, A.W. (Ed.), Atlas of Seismic Stratigraphy I. : Studies in Geology, vol.27. American Association of Petroleum Geologists, pp. 1–10.
Vail, P.R., Audemard, F., Bowman, S.A., Eisner, P.N., Perez-Cruz, C., 1991. The Stratigraphic Signatures of Tectonics, Eustasy and Sedimentology — An Overview. In: Einsele, G., Ricken, W., Seilacher, A. (Eds.), Cycles and Events in Stratigraphy. Springer-Verlag, Berlin, pp. 617–659.
Van der Zwan, C.J., 1990. Palynostratigraphy and palynofacies reconstruction of the Upper Jurassic to Lowermost Cretaceous of the Draugen Field, offshore Mid Norway. Review of Palaeobotany and Palynology 62 (1–2), 157–186.
Wang, P., Cheng, X., 1985. Distribution of Calcareous Nannofossils in the East China Sea. In: Wang, P. (Ed.), Marine Micropaleontology of China. Springer-Verlag, Berlin, pp. 218–228.
Whitaker, M.F., 1984. The Usage of Palynostratigraphy and Palynofacies in Definition of Troll Field Geology. In: Reduction of Uncertainties by Innovative Reservoir Geomodeling. Vol. Paper G6. 6th Offshore Northern Seas Conference and Exhibition, Stavanger 1984, Norsk petroleums-forening, Norway, p. 44.